INL/RPT-23-73207
Revision 0

Advanced Reactor Technologies: Gas-Cooled Reactor First Quarter 2023 Report

October, November, and December 2023

Paolo Balestra, William E Windes, Ting-Leung Sham, John D Stempien

Idaho National Laboratory

INL is a U.S. Department of Energy National Laboratory
operated by Battelle Energy Alliance, LLC

INL/RPT-23-73207
Revision 0

Advanced Reactor Technologies: Gas-Cooled Reactor First Quarter 2023 Report

October, November, and December 2022

Idaho National Laboratory
INL ART Program
Idaho Falls, Idaho 83415

http://www.inl.gov

Prepared for the
U.S. Department of Energy
Office of Nuclear Energy
Under DOE Idaho Operations Office
Contract DE-AC07-05ID14517

Page intentionally left blank

INL ART Program

Advanced Reactor Technologies: Gas-Cooled Reactor First Quarter 2023 Report

INL/RPT-23-73207

Revision 0

October, November, and December 2022

Approved by:

Travis Mitchell — 6/12/2023

Travis R. Mitchell
INL ART Program Manager

Date

Page intentionally left blank

CONTENTS

FIGURES

TABLES

Page intentionally left blank

ACRONYMS

AGC	Advanced Graphite Creep
AGR	Advanced Gas Reactor
AL	Analytical Laboratory
ANL	Argonne National Laboratory
ANS	American Nuclear Society
ART	Advanced Reactor Technologies
ASME	American Society of Mechanical Engineers
ASTM	American Society for Testing and Materials
ATR	Advanced Test Reactor
BPVC	Boiler and Pressure Vessel Code
CAES	Center for Advanced Energy Studies
CCCTF	Core Conduction Cooldown Test Facility
CTE	Coefficient of thermal expansion
DCPD	Direct current potential drop
DIC	Digital Image Correlation
DOE	Department of Energy
EPP	Elastic perfect plastic
EPRI	Electric Power Research Institute
FBCVD	Fluidized bed chemical vapor deposition
FFC	Fuel and Fuel Cycle
FITT	Furnace for Irradiated TRISO Testing
FY	Fiscal Year
GCCCCA	Graphite and Ceramic Composite Core Components and Assemblies
GIF	Generation IV International Forum
HFEF	Hot Fuel Examination Facility
HFIR	High-Flux Isotope Reactor
HTGR	High-temperature gas-cooled reactor
HTR	High-temperature reactor
HTTF	High-Temperature Test Facility
HTTR	High-Temperature Test Reactor
IAEA	International Atomic Energy Agency
IMCL	Irradiated Materials Characterization Laboratory
IMGA	Irradiated Microsphere Gamma Analyzer

INL	Idaho National Laboratory
IPyC	inner pyrolytic carbon
IRC	INL Research Center
JAEA	Japan Atomic Energy Agency
LBL	leach-burn-leach
LIBS	Laser-Induced Breakdown Spectroscopy
LOFC	loss-of-forced-cooling
MFC	Materials and Fuels Complex
MiNES	Materials in Nuclear Energy Systems
MOOSE	Multiphysics Object Oriented Simulation Environment
MR&D	Materials Research & Design, Inc.
NDE	Non-destructive examination
NDM	Non-metallic Design and Materials
NDMAS	Nuclear Data Management and Analysis System
NEA	Nuclear Energy Agency
NEAMS	Nuclear Energy Advanced Modeling and Simulation
NEI	Nuclear Energy Institute
NGKB	Nuclear Graphite Knowledge Base
NQA	Nuclear Quality Assurance
NRAD	Neutron Radiography
NRC	Nuclear Regulatory Commission
NSTF	Natural Convection Shutdown Heat-Removal Test Facility
OECD	Organization for Economic Co-operation and Development
ORNL	Oak Ridge National Laboratory
OPyC	Outer pyrolytic carbon
PC	Personal computer
PGS	Precision gamma scanner
PIRT	Phenomena Identification and Ranking Table
PMB	Project Management Board
POF	Probability of failure
R&D	Research and development
RCCS	Reactor Cavity Cooling System
RIM	Reliability and Integrity Management
Rtf	Ratio of flexural to tensile strength
SEM	Scanning electron microscope

SiC	Silicon carbide
TAVA	Time-averaged, volume-averaged
TCM	Thermal Conductivity Microscope
TECDOC	Technical document
TEM	Transmission electron microscopy
TGA	thermogravimetric analyzer
TMS	The Minerals, Metals & Materials Society
TOF	Time of flight
TRISO	Tristructural isotropic
UCO	Uranium carbide/oxide
UK	United Kingdom
US	United States
USNC	Ultra Safe Nuclear Corporation
VHTR	Very-high-temperature reactor
WG	Working group
XCT	X-ray computed tomography
XRF	X-ray fluorescence

Page intentionally left blank

Advanced Reactor Technologies:
Gas-Cooled Reactor First Quarter 2023 Report

1. MAJOR ACCOMPLISHMENTS

1.1 Fuels Development

Highlights of Advanced Gas Reactor (AGR) fuels-development activities during October, November, and December 2022 are as follows:

October

- Initiated rebuilding of the Fuel Accident Condition Simulator (FACS) furnace at Idaho National Laboratory (INL). Awaiting arrival of new thermocouples to complete the rebuild.
- Initiated work on a furnace for use in the Neutron Radiography (NRAD) Reactor at INL to screen AGR-5/6/7 Capsule 1 compacts for particle failures. Use of a radiography beamline as a neutron source has been ruled out due to insufficient flux. Transfer and handling is going to be a significant issue given limited headroom above the NRAD pool. Alternative potential solutions that will be pursued include employing the Transient Reactor Test (TREAT) Facility at INL.
- Completed transfer of two AGR-5/6/7 compacts to the Analytical Laboratory (AL) at INL for deconsolidation leach-burn-leach (LBL) analysis.
- Initiated gamma tomography of the AGR-5/6/7 Capsule 1 fuel holder at INL.
- Completed second shipment of AGR-5/6/7 compacts (Compacts 1-5-9, 2-3-2, 5-5-3, and 4-1-3) from INL to Oak Ridge National Laboratory (ORNL).
- Hosted Department of Energy (DOE) Federal Program Manager Matthew Hahn at INL for facility tours and meetings with Advanced Reactor Technologies (ART) staff.
- Initiated 1600°C safety test of AGR-5/6/7 Compact 5-5-3 in the ORNL Core Conduction Cooldown Test Facility (CCCTF).
- Completed burn-leach of the graphite holder used in the AGR-5/6/7 Compact 2-2-4 1600°C safety test at ORNL.
- Completed deconsolidation and preburn leaching at ORNL of 1600°C safety-tested AGR-5/6/7 Compact 2-2-4, and separated tristructural isotropic (TRISO) particles from matrix debris for irradiated microsphere gamma analyzer (IMGA) survey.
- Completed four-hour gamma counting of 45 randomly selected TRISO particles deconsolidated from AGR-5/6/7 Compact 2-2-2 using the ORNL IMGA.
- Completed preparation of polished cross sections and optical microscopy of particles representing various levels of silver retention deconsolidated from as-irradiated AGR-5/6/7 Compact 2-2-1.
- Attended 6th Workshop on Material Properties of TRISO Fuels organized and chaired by Tyler Gerczak (of ORNL) and held in conjunction with the Generation IV International Forum, Very High Temperature Reactor Systems Fuel and Fuel Cycle Project Management Board annual meeting, in which presentations were given by ORNL and INL AGR program staff on a broad range of topics.
- Published a paper in the Journal of Nuclear Materials on “Microstructure of Irradiated Buffer Layers as Measured by X-Ray Computed Tomography,” *J. Nucl. Mater.* 572 (2022) 154061.

- Published paper in Journal of Nuclear Materials on "AGR-2 Irradiated TRISO Particle IPyC/SiC Interface Analysis Using FIB-SEM Tomography," *J. Nucl. Mater.* 573 (2022) 154104.

November

- Completed gamma tomography of the AGR-5/6/7 Capsule 1 fuel holder at INL using the Precision Gamma Scanner and generated preliminary reconstructed images.
- Completed acid leaching of the metallic hardware from AGR-5/6/7 Capsules 2 and 5 at INL. This concludes the acid leaching of all the irradiation test train metallic hardware. The solutions will be analyzed for gamma-emitting fission products and beta-emitting Sr-90.
- Performed sectioning, grinding, polishing, and optical microscopy of cross sections of AGR-5/6/7 Compacts 1-7-1, 1-7-6, 3-2-3, and 4-5-1.
- Completed transfer to the Hot Fuel Examination Facility of particles deconsolidated from AGR-5/6/7 Compacts 1-7-4 and 1-7-9 for ceramographic sample preparation at INL.
- Completed 1600°C safety test of AGR-5/6/7 Compact 5-5-3 in the ORNL CCCTF.
- Completed 50 h, 1400°C inert gas heating test in the ORNL Furnace for Irradiated TRISO Testing (FITT) using full TRISO particles from as-irradiated AGR-5/6/7 Compact 2-2-1.
- Completed a 400 h FITT oxidation test, in which TRISO particles deconsolidated from as-irradiated AGR-5/6/7 Compact 2-2-1 were heated at 1400°C in a flowing 2% O_2 atmosphere.
- Completed short-count (60 s) survey with the ORNL IMGA of burned-back particles deconsolidated from AGR-5/6/7 Compact 2-2-2 safety-tested at 1600°C.
- Completed short-count (60 s) survey with the ORNL IMGA of full TRISO particles deconsolidated from 1600°C safety-tested AGR-5/6/7 Compact 2-2-4.
- Completed deconsolidation and preburn leaching of as-irradiated AGR-5/6/7 Compact 1-5-9 and particles are being hand sorted with the ORNL Particle Microsphere Manipulator before IMGA survey to separate out particles most affected by nickel degradation.

December

- Completed deconsolidation-LBL of AGR-5/6/7 Compact 5-1-2 at INL.
- Completed a Level 2 milestone at INL for the shipment of four AGR-5/6/7 fuel compacts from INL to ORNL. So far there have been three shipments of compacts from INL to ORNL.
- Completed first rounds of grinding, polishing, and optical microscopy on mounts of cross-sectioned AGR-5/6/7 Compacts 1-7-1, 1-7-6, 3-2-3, and 4-5-1 at the Hot Fuels Examination Facility (HFEF) at INL.
- Completed acid leaching of metallic hardware from all AGR-5/6/7 Capsules at HFEF at INL. The final two to be leached were Capsules 2 and 5 in December.
- Completed gamma tomography on the AGR-5/6/7 Capsule 1 graphite holder using the precision gamma scanner (PGS) at INL.
- Completed axial scanning of the AGR-5/6/7 Capsule 5 graphite holder via PGS at INL.
- Completed evaluation of deposition cups from 1600°C safety test of AGR-5/6/7 Compact 5-5-3 in the ORNL CCCTF, and no appreciable cesium radionuclides were detected, which is consistent with zero particle failure seen in previous two tests of Capsule 2 compacts at 1600°C.

- Completed first 1800°C safety test of an AGR-5/6/7 compact (Compact 2-3-2) in the ORNL CCCTF, and results of monitoring for release of krypton and cesium radionuclides indicated elevated release from two or three particles.
- Completed short-count (60 s) survey with the ORNL IMGA of all TRISO particles deconsolidated from as-irradiated AGR-5/6/7 Compact 1-5-9 as part of study to identify and examine particles degraded by nickel infiltration from adjacent thermocouple in the irradiation test capsule.
- Completed long-count (4 h) gamma counting with the ORNL IMGA of 45 randomly selected TRISO particles deconsolidated from 1600°C safety-tested AGR-5/6/7 Compact 2-2-4 for further evaluation of radionuclide retention and selection of representative particles for microanalysis. Previous short-count (60 s) survey of all particles verified that no particles exhibited degradation of the normal high-retention properties of the coatings.
- Completed materialographic sample preparation at ORNL of representative TRISO particles selected from AGR-5/6/7 Compact 2-2-2, and completed optical microscopy of polished cross sections.
- Completed installation of new scanning electron microscope (SEM) to replace aging instrument used at ORNL for microstructural analysis of AGR-1 and AGR-2 irradiated particles.

1.2 High-Temperature Materials Development

Highlights of high-temperature materials activities during October, November, and December 2022 are as follows:

October

- Sustained the long-term creep-rupture test (800°C, 35 MPa) of an Alloy 617 base-metal V-notch specimen. The expected life is 100,000 hours. The test is currently at 40,100 hours.
- Sustained a long-term creep-rupture test (800°C, 35 MPa) of an Alloy 617 weld-metal V-notch specimen. The expected life is 100,000 hours. The test is currently at 11,200 hours.
- Sustained a creep-rupture test (850°C, 63 MPa) of an Alloy 617 base-metal specimen comprised of two V-notches. The test is currently at 4,300 hours.
- Sustained creep-rupture testing (800°C, 65 MPa) of an Alloy 617 uniaxial specimen. The test is currently at 4,200 hours. The test will be interrupted periodically in an attempt to identify the best shutdown and restart procedure.
- Sustained creep-rupture testing (800°C, 65 MPa) of an Alloy 617 uniaxial specimen. The test is currently at 3,800 hours. The test will be interrupted periodically in an attempt to identify the best shutdown and restart procedure.
- Attended the G4SR-4 Meeting and presented on the ART material-qualification work on a panel in the Nuclear Material Challenges for Small Modular Reactors and Advanced Reactors Workshop.
- Determined necessary attributes for a crack-opening displacement gauge to be ordered and paired with current direct current potential drop (DCPD) capabilities for crack-growth measurements.
- Compiled crack-growth testing matrix of Alloy 617 in air, in accordance with American Society for Testing and Materials (ASTM) 1457 and ASTM 2760.

- Continued assessment of proposed Class B code case with the pressurized simplified-model test (p-SMT) with Alloy 617 material and pressurized tube with material stainless steel (SS)316 against proposed Class B.
- Made repairs to computers and a hydraulic pump to allow for continued cyclic testing. Hydraulic pump repairs include the replacement of a heat exchanger and flushing the oil lines to remove water that leaked from the failed heat exchanger.

November

- Long-term very-high-temperature reactor (VHTR) material qualification—INL
  - Alloy 617 double V-notch test at 850°C, 63 MPa was completed.
  - Maintained weld-metal alloy 617 V-notch test (800°C, 35 MPa), current test time is 11,900 hours.
  - Maintained base-metal alloy 617 V-notch test (800°C, 35 MPa), current test time is 40,809 hours.
  - Maintained creep-rupture testing of an Alloy 617 uniaxial specimen (800°C, 65 MPa). The test is currently at 5,066 hours. The test will be interrupted periodically in an attempt to identify the best shutdown and restart procedure.
  - Maintained creep-rupture testing of an Alloy 617 uniaxial specimen (800°C, 65 MPa). The test is currently at 4,654 hours. The test will be interrupted periodically in an attempt to identify the best shutdown and restart procedure.
  - Used laser ultrasound to measure the elevated-temperature properties for the Alloy 800H base plate and UTP 2133 Mn filler metal. The UTP 2133 Mn filler metal showed a reduced elastic modulus and lower Poisson's ratio than the Alloy 800H.
  - Performed SEM to confirm that the interdendritic segregation seen in optical microscopy was a result of the high niobium concentration (1.23 wt%) in the UTP 2133 Mn filler metal.
  - Ordered extensometer for load-line displacement measurements to enable creep-crack growth-rate testing.
  - Redesigned compact tension specimens for creep-crack growth testing to meet ASTM standards for this type of test.

December

- High-temperature design methodology—INL
  - Work on the task to revamp the ASME Section III, Division 5, Class B design rules continued. A list of candidate Class B materials was established. Researched ASME Section II materials and ASME ST LLC sponsored research and development (R&D) work to identify data gap for the new Class B materials. Evaluated the time extrapolation procedure developed in Fiscal Year (FY)-22 for Class B allowable stresses. Developed a draft code case outline for the new Class B rules.
  - Ting-Leung Sham attended the North American Advanced Reactor Codes & Standards Workshop in Washington DC and gave a presentation entitled, "ASME Section III, Division 5, High Temperature Reactors, High Temperature Materials."
- Long-term VHTR material qualification-INL
  - Remeasured and analyzed the coefficient of thermal expansion (CTE) for Alloy 800H and the UTP 2133 Mn filler metal due to issues with the previous tests. The Alloy 800H and UTP 2133 Mn CTE data are now in close agreement and similar to prior CTE data published for Alloy 800H.
  - Maintained weld-metal alloy 617 V-notch test (800°C, 35 MPa), current test time is 12,598 hours.
  - Maintained base-metal alloy 617 V-notch test (800°C, 35 MPa), current test time is 41,506 hours.

- Maintained creep-rupture testing of an Alloy 617 uniaxial specimen (800°C, 65 MPa). The test is currently at 9,099 hours. The test will be interrupted periodically in an attempt to identify the best shutdown and restart procedure.
- Maintained creep-rupture testing of an Alloy 617 uniaxial specimen (800°C, 65 MPa). The test is currently at 8,260 hours. The test will be interrupted periodically in an attempt to identify the best shutdown and restart procedure.

1.3 Graphite

Highlights of graphite activities during October, November, and December 2022 are as follows:

October

- Transferred the highest-activity AGC-4 samples into the Materials and Fuels Complex (MFC) AL hot cells for survey and handling. The samples have been individually packaged to control potential cross-contamination. A radiological standard has been prepared to allow consistent, precise measurements to be made using the Hot Cell 4 gamma spectrometer.
- Fabricated specialized quartz containers to allow oxidation of identified high-activity samples in the Hot Cell 5 box furnace and allow measurement of beta-emitting isotopes such as nickel-63. After oxidation, the residue will be dissolved in acid, and the solution measured using beta proportional counting and mass spectrometry.
- Presented an overview of AGC-4 work at MFC AL to DOE program-management visitor, Matthew Hahn.
- Decontaminated AGC-4 flux wires at CFA-625, Lab 240, and are awaiting measurements when instrument time becomes available.
- Initiated collaboration with ORNL to develop methods for uncertainty quantification and standards development for consistency in detector measurements through the interpretation and improvement of ASTM standards.
- Abstract on semiempirical modeling of dimensional change in nuclear graphite has been accepted for poster presentation at The Minerals, Metals & Materials Society (TMS).
- Abstract on semiempirical modeling of dimensional change in nuclear graphite has been accepted for a paper for publication in the ASME Pressure Vessels & Piping Conference.
- Published paper: S. Johns, T. Yoder, K. Chinnathambi, R. Ubic, W.E. Windes, "Microstructural changes in nuclear graphite induced by thermal annealing," *Materials Characterization* 194, December 2022, 112423, https://doi.org/10.1016/j.matchar.2022.112423.
- Received peer review comments on a manuscript entitled "High Temperature Annealing of Irradiated Nuclear Grade Graphite." The revised manuscript will be submitted to the *Journal of Nuclear Material* on or before November 19, 2022.
- Presented semiempirical model on irradiated graphite behavior in the Vendor Irradiation Capsule Workshop at ORNL on October 4, 2022.
- Ordered a Gatan Model 652 *in situ* heating holder for the Spectra transmission electron microscope (TEM) at Center for Advanced Energy Studies (CAES).
- Received 19 new desktop computers for the Carbon Characterization Laboratory upgrade. These computers have been imaged and Microsoft Office has been installed. All of them have been configured and are ready for custom software installation.
- Provided final typeset proofs to authors for approval of chapters for the ASTM Selected Technical Paper (STP) Volume "Graphite Testing for Nuclear Applications: The Validity and Extension of Test

Methods for Material Exposed to Operating Reactor Environments." Publication is expected in November 2022.

- Held first (virtual) task-group meeting of newly formed ASME Nonmetallic Component Degradation and Failure Monitoring Task Group set up through Section III, but administered by Section XI Reliability and Integrity Management (RIM) on October 17, 2022. This task group, chaired by Dr. M. Metcalfe, will address graphite RIM requirements in the ASME code, with other nonmetallics to be considered later. A second meeting with an expanded membership will be held in early December. The task group will consider, as a first stage, the fitness for purpose of a prepared draft document, to be offered to Section XI, that focuses on RIM requirements for gas-cooled high-temperature reactor (HTR) designs.
- Submitted a charter proposal for this ASME Nonmetallic Component Degradation and Failure Monitoring Task Group to the chair of the RIM Section XI Subgroup for approval at the November ASME Code Week.
- Approved ASME ballot for text changes to ASME Section III Design Code by the Nonmetallics Working Group concerning nuclear-graphite component damage. These changes address functionality and damage-tolerance terms and ambiguities around the use of the term probability of failure (POF). They will now progress to the next ASME administrative level for approval.
- Attended ASME Section III Design Task Group virtually, October 20, 2022.
- Submitted a paper entitled "Damage Tolerance in the Graphite Cores of United Kingdom (UK) Power Reactors and Implications for New Build," by M. P. Metcalfe the journal *Nuclear Engineering and Design*. The paper is currently undergoing peer review. This paper has been commissioned as a supporting reference to the ASME Section III design code.
- Held the fourth quarterly meeting for Working Group (WG) on General Requirements for Graphite and Ceramic Composite Core Components and Assemblies (GCCCCA) virtually on October 31, 2022, per WG member request. Future meetings will align with the ASME Boiler Pressure Vessel Code (BPVC) week meetings. The draft minutes and meeting presentations will be distributed during November.
- Held a Composite Task Group meeting on Oct 27, 2022. The focus for this meeting was on material vs component modeling and the application during design. The topic was presented by Materials Research & Design, Inc. (MR&D), with very good questions and observations from the community in context of the ASME code.
- Worked changes to ASME Record 20-1307 (proposal for carbon-carbon [C C] nonmandatory appendices) to be presented at Sec III during code week, scheduled on Nov 10th, 2022. Record 22-1463, which clarifies the roles and responsibilities of nonmetallic core components, passed the working group review and needs to be balloted for the next-level review to the subgroup General Requirements for approval. WG Nonmetallic and Design as well as subgroup High Temperature Reactors will be able to comment.
- Hosted the ORNL/INL "Commercial Graphite Irradiation Capsule Workshop" at ORNL, October 3–4, 2022. About 41 people, representing 19 different companies or entities, attended (in person or virtually) the workshop. Advanced-reactor companies in attendance included FLiBe Energy, Kairos Power, Radiant Nuclear, Ultra Safe Nuclear Company (USNC), Westinghouse, X-Energy, and Framatome. Graphite manufacturers included Amsted Graphite Materials, Ibiden, Mersen, SGL Carbon, Tokai Carbon, and Toyo Tanso. The remaining representatives included ORNL, INL, Jacobs, MWI, Inc., National Nuclear Laboratory, and the University of Manchester. During the workshop, presentations and discussions were held regarding the needs of the reactor designers and how their

different needs can overlap for cost-sharing in upcoming irradiation experiments. A report will follow.

- Held a joint ORNL/INL meeting of the ART Graphite Program at ORNL, October 5–6, 2022. This was the first in-person meeting of the program. Participants from ORNL and INL presented overviews of the various activities and discussions were held about future work and areas of collaboration.
- Prepared a set (10 samples in total) of graphite discs for split-disc testing from graphite grade IG-110. The samples are being compression tested according to ASTM D8289-20 Standard, "Test Method for Tensile Strength Estimate by Disc Compression of Manufactured Graphite," with dissolved inorganic carbon (DIC) measurement integrated. The data collected will be analyzed and compared with previous results obtained using graphite grade Mersen 2114.
- Polished PCEA samples of three different batches to perform elastic property measurements as well as microscopy characterization.
- Submitted manuscript "Small Size Graphite Disc Compression Test and DIC Full Field Measurement" to the journal *Carbon.* It is currently under review.
- Attended the Nuclear Materials Conference (NuMAT) 2022 and presented an invited talk titled "Utilizing X-Ray Diffraction and Williamson-Hall Analysis to Quantify Microstructural Changes in Irradiated Nuclear Graphite."
- Submitted a Rapid Turnaround Experiment proposal called "Microstructural characterization of neutron-irradiated C-C composites" to characterize the irradiation effects in C-C composites.

November

- Characterized 60 creep samples for gross gamma-count rate and confirmed that less than half of samples have dose rates in excess of values that could be handled individually at the INL Research Center (IRC).
- Made provisions for performing dimensional measurements of low-activity samples in a hood at MFC AL as part of decontamination and final dose-rate checks.
- Completed 95% of Baseline Characterization Database Verification Report for PCEA Billet 02S8-5.
- Completed 90% of Baseline Characterization Database Verification Report for PCEA Billet 01S8-9.
- Installed custom data acquisition software on six personal computers (PCs) in support of the Carbon Characterization Laboratory upgrade.
- Networked six PCs to the main server computer in support of the Carbon Characterization Lab upgrade.
- Wrote custom software to communicate with a new Mettler balance in IRC Lab C-20 for oxidation studies.
- Devised a simplified version of the graphite-analysis tool for filtering and downloading graphite data.
- Attended the fourth quarterly meeting of the ASME WG Nonmetallic Design and Materials (NDM) held in Pittsburgh, Pennsylvania, on Nov 1, 2023. The draft minutes and meeting presentations will be distributed during December.
- Passed final review on several records and the changes are *en route* for publication in the ASME BPVC 2023 edition. This includes records 20-1307 (proposal for C-C nonmandatory appendices), 20-1308 (simple assessment and Weibull notations, which also includes the split-off errata record 20-2099) and R21-728 (HHB corrections). All listed records were approved by Sec III by the second

iteration review. Record 22-516 (Intent on historical use) was revised and recirculated for Sec III review. Record 22-1463 to clarify the roles and responsibilities was prepared for next-level review to subgroup General Requirements for approval. Working group Nonmetallic and Design as well as subgroup High-Temperature Reactors will be able to comment.

- Received first draft report from MR&D and began the review. It will support the final report to address the initial analysis that was performed for Sec III, Div. 5, Subsection HH, Subpart B.
- Participated in several task group meetings now occurring on regular basis, including: the Composites Task group, Nonmetallic Component Degradation and Failure Monitoring Task Group (official ASME Task group under Sec XI), and the Design Task Group. In addition, there are also activities from the Molten Salt and Irradiation Task Groups that are occurring on an *ad hoc* basis.
- Attended in-person meetings of ASME Code Week in Pittsburgh, Pennsylvania, November 6–8, 2022. This included attendance of the Monitoring and Nondestructive Examination (MANDE (Monitoring and NDE) Working Group on Sunday, November 6, the Section XI, Div.2 RIM Subgroup and Weibull/POF Task Group on November 7, and the Section III Nonmetallics Working Group on November 8, 2022.
- Held virtual ASTM D02.F Subcommittee meetings on November 21–22, 2022. ORNL had significant participation. Some actions involved the revision of ASTM C559, "Standard Test Method for Bulk Density by Physical Measurements of Manufactured Carbon and Graphite Articles"; involvement also included the discussion of permeability measurements of graphite and developing of standards related to molten-salt effects on graphite.
- Attended the annual Technical Meeting of the International Atomic Energy Agency (IAEA) Nuclear Graphite Knowledge Base (NGKB), held in Vienna, Austria, November 28–30, 2022. ORNL researcher N. Gallego is the chair of the Committee. The IAEA NGKB is the storehouse for much of the historical nuclear graphite data available from numerous countries including the United States (US), European Union, UK, Russia, and elsewhere. Among the various topics discussed at the meeting, included: integration of the information in the knowledge base to the Generation IV International Forum (GIF) Handbook; integration of the ART Nuclear Data Management and Analysis System (NDMAS) database to the IAEA NGKB; publication of two technical documents (TECDOCs) (one on creep and one on graphite oxidation) that have been on the IAEA pipeline for several years; and potential expansion of the committee to include topics related to graphite-waste management. Unfortunately, on the topic of publications, the IAEA continues to cite plagiarism in the TECDOC related to graphite oxidation (or burning), despite DOE's and INL's communication and approval to use content of a previously published INL report, and it is recommending significant re-writing of the report. Based on this input, a decision to withdraw this document from the IAEA publication system was taken by the INL authors. The Creep TECDOC will be resubmitted next to the IAEA publications committee.
- Completed initial analysis of the DIC data for the ten small-size IG-110 graphite-disc compression tests. Analysis and comparisons from experiments and simulations for graphite grade IG-110 and Mersen 2114 will continue.
- Started characterization of PCEA specimens using helium pycnometry, mass, and dimensional inspections. These measurements are being conducted to understand the differences between batches of graphite and decide how historical data can be used to support material qualifications.
- Commenced preparation of samples of IG-110, NBG-18, PCEA, and 2114 for characterization via mechanical polishing serial-sectioning using optical microscopy. These data are being acquired to support the library of microstructures at ORNL and image-based modeling activities.

- Finished stage and sample preparations as part of the proposal "In-situ oxidation [x-ray computed tomography] XCT microstructural analysis of nuclear graphite." The experiments will be performed at the Diamond Light Source (UK), December 8–12, 2022.
- Started literature review on helium gas flow in high-temperature graphite reactors. The key parameters of helium-gas flow in graphite channels, such as mass flow rate, density, viscosity, velocity, channel-section area, etc., are being collected to design gas-erosion tests on graphite.
- Published article "SEM and TEM data of nuclear graphite and glassy carbon microstructures" in *Data in Brief*, available at https://doi.org/10.1016/j.dib.2022.108808. This publication is part of the milestone in microstructural characterization to build a database of nuclear-graphite characteristics.
- Published invited paper, titled "Perspective on 'code qualifying' new graphite grades for use in advanced nuclear reactors," in the "Rising Stars in Nuclear Materials: 2022" special issue in *Frontiers in Nuclear Engineering*. The article is open-access and available at https://doi.org/10.3389/fnuen.2022.1045607.
- Received comments from journal peer review of the manuscript "Small Size Graphite Disc Compression Test and DIC Full Field Measurement." Efforts to address comments from reviewers are ongoing. The manuscript will be resubmitted to the journal *Carbon*.
- Submitted the article "Microstructural characterization of the CGB graphite grade from the molten salt reactor experiment" to the *Journal of Nuclear Materials* for review.

December

- Hosted visitors from Kairos Power for a tour of graphite-characterization and oxidation labs at IRC. Discussed work practices and quality assurance, identifying complementary efforts among capabilities suitable for testing both irradiated and virgin graphite materials.
- Attended Electric Power Research Institute (EPRI) and Nuclear Energy Institute (NEI) Advanced Reactor Roadmap and Standards Workshop (December 1, 2022).
- Participated in ASTM D02.f committee meetings. Strategies are under development for addressing historical ASTM non-compliant (according to updated ASTM regulations) standards to prevent their withdrawal.
- Completed the first draft of the paper, "Semi-empirical modeling of irradiation-induced dimensional change in nuclear graphite H-451," for publication in the ASME Pressure Vessels & Piping Conference.
- Developed a test matrix for a comparison study of X-ray diffraction and Raman to define the limitations of both techniques.
- Sent ASME Record 22-1463 (to clarify the roles and responsibilities) for review and approval to subgroup General Requirements and for comment and review to subgroup High-Temperature Reactors and WG NDM.
- Attained ASME Administrative Board approval of the following records, and the updates will be published in the 2023 edition: 20-1307, Proposal for C-C nonmandatory appendices; R21-728, On HHB corrections; 22-516, Intent on historical use; 21-1392, On oxidation; 22-487, On G-certificate and GC certificate-holder clarifications; 19-2805, Eliminate use of historical dose units; and 20-1308, Simple assessment and Weibull notations, which also includes the split-off errata record 22-2099).
- Held the second meeting of the ASME Task Group on Nonmetallic Component Degradation and Failure Monitoring, discussing the mission statement of the group and how the work of this task group does and does not overlap with the Section III working group.

- Convened the ASME Design Task Group meeting, discussing needs related to the full assessment of the graphite POF. Changes from the 2019 to the 2021 code versions have caused uncertainty in how to implement the POF calculations. Also, the group would like to develop a more-realistic definition of the V_m parameter while remaining conservative, but not having V_m be so small as to prevent POF calculation from being performed for ultrafine-grain graphite grades.
- Provided ASME Design Task Group with unirradiated and irradiated baseline program data through Box (also directed group participants to the NDMAS portal).
- Started development of memorandum to Nuclear Regulatory Commission (NRC) on the relative conservatism of full and simplified POF assessments. Collaborating with MPR Associates and Ultra Safe Nuclear Corporation (USNC) to validate POF results and duplicate baseline program finite-element models.
- Started analysis on mesh convergence with a paper to publish the results.
- Conducted *in situ* oxidation, coupled with XCT experiments, at the Diamond Light Source (UK). These experiments were conducted to understand real-time degradation (oxidation) of graphite under accident conditions, leading to air ingress into the reactor. The graphite grades that were evaluated included PCEA, IG-110, and NBG-18.
- Completed a second round of review and revision of a manuscript related to split-disc testing coupled with DIC analysis. The manuscript title was revised as "Mechanical Behavior Analysis Using Small-Size Graphite Disc Compression Testing with Digital Image Correlation Methods" and is planned for resubmission to *Carbon* in January 2023.
- Completed comprehensive data analysis of IG-110 small-size disc compression tests, including load-displacement history, DIC strain measurement, analytical calculation, and FE simulation. The initial results show some differences in mechanical behavior during the compression between graphite grades IG-110 and Mersen 2114.
- Completed the order of DIC product (Correlated Solutions, VIC-3D) to continue support of DIC studies coupled with split disc testing.
- Initiated efforts to compile ORNL reports that cover the neutron spectrum and flux and fluence reporting for the Oak Ridge Research Reactor. The objective is to obtain a better quantification of the neutron doses reported for graphite creep experiments carried out on H-451 that have been published in the open literature.
- Finished with Baseline Characterization Database Verification Report for PCEA Billet 02S8-5 and submitted to INL review system.
- Finished with Baseline Characterization Database Verification Report for PCEA Billet 01S8-9 and submitted to INL review system.
- Published several contributions in the ASTM International book on the Selected Technical Papers (STP 1639) *Graphite Testing for Nuclear Applications: The Validity and Extension of Test Methods for Material Exposed to Operating Reactor Environments* (ISBN:978-0-8031-7725-3). The book provides peer-reviewed documentation of materials presented at the ASTM symposium held virtually September 23–24, 2021:
  - "Equibiaxial Flexure Strength of a Superfine-Grained Nuclear Graphite," available at http://doi.org/10.1520/STP163920210075.
  - "Effects of Microstructural Composition, Porosity, and Microcracks on the Elastic Moduli of Nuclear Graphites," available at http://doi.org/10.1520/STP163920210073.
  - "Evaluating the Effects of Molten Salt on Graphite Properties: Gaps, Challenges, and Opportunities," available at http://doi.org/10.1520/STP163920210103.

  - "A Microstructural Modeling-Based Approach to Graphite Oxidation beyond ASTM D7542," available at http://doi.org/10.1520/STP163920210080.
  - "Performance of Graphite Oxidation with Environment and Specimen Geometry Variations," available at http://doi.org/10.1520/STP163920210134.
- Achieved acceptance for publication of the article "Codes and Standards for Ceramic Composite Core Materials for High-Temperature Reactor Applications" in the journal *Nuclear Engineering and Design*.
- Achieved acceptance for publication of the paper "On the thermal oxidation of nuclear graphite relevant to high-temperature gas-cooled reactors" in the *Journal of Nuclear Materials*.
- Submitted a paper to the journal *Nuclear Technology and Design*: "Damage Tolerance in the Graphite Cores of UK Power Reactors and Implications for New Build," which is currently undergoing peer review. This paper is intended as a reference on damage tolerance for the ASME BPV Section III, Division 5, Design Code for high-temperature reactors.
- Prepared the paper "Initial analysis of the ASME Code Rules for Subsection III-5-HHB (Composite Materials) for current HTR Design Requirements" to be presented at the 47th International Conference and Expo on Advanced Ceramics and Composites (ICACC 2023), to be held in Daytona Beach, FL, January 22–27, 2023.
- Submitted three abstracts on nuclear graphite research at ORNL to *Carbon 2023*, the World Conference on Carbon, to be held in Cancun, Mexico, July 16–21, 2023.

1.4 Methods Modeling and Validation

Highlights of methods modeling and validation activities during October, November, and December 2022 are as follows:

October

- Reviewed the HTTR journal paper internally for submission.
- Finalized initial draft of HTTR M&C conference paper.
- Drafted A Journal paper for submission to Annals of Nuclear Energy with title "High-Fidelity Monte Carlo based simulation of a Pebble Bed Reactor the Run-In phase."
- Continued work on draft benchmark specifications.
- Developed PG-29 calibration tools.
- Performed preliminary PG-29 calibrations.
- Confirmed Nuclear Quality Assurance (NQA)-1 audit of Natural Convection Shutdown Heat-Removal Test Facility (NSTF) Quality Assurance Program Plan for February 2022 by INL NQA-1 Lead Auditor.
- Continued NSTF matrix testing including x3 blocked riser channels in DataQuality080.

November

- Presented four papers at the 2022 American Nuclear Society (ANS) Winter Meeting in Phoenix, AZ:
  - "Methodology for Determining the Run-In Scenario for a Pebble Bed Reactor"
  - "Discrete Element Method Investigation of Reflector Dimples for a General Pebble Bed Reactor Design"

  - "Gas Cooled Reactor Equilibrium Core Calculations Using Nuclear Energy Advanced Modeling and Simulation (NEAMS) Tools"
  - "Determination of an Initial Critical Fuel Height for a Pebble-Bed Reactor"
- Submitted a journal paper to Annals of Nuclear Energy with the title "Discrete Element Simulation of Pebble Bed Reactors on Graphics Processing Units." The comments from two reviewers were addressed by adding a sensitivity study on the dimension of the pebble-bed dimples.
- Submitted a journal paper, "Discrete Element Simulation of Pebble Bed Reactors on Graphics Processing Units." to *Annals of Nuclear Energy*.
- Submitted a journal article, "Improved Multiphysics Model of the High Temperature Engineering Test Reactor for the Simulation of Loss-of-Forced-Cooling Experiments," to *Annals of Nuclear Energy*.
- Attended the ANS Winter meeting in Phoenix, AZ. The NSTF team presented a paper entitled "Modeling of a Large Scale Reactor Cavity Cooling System (RCCS) Operating at Two-Phase Transient Conditions with RELAP5-3D," and spoke on the Thermal Hydraulics Issues in Licensing of Advanced Reactors panel session.
- Ratified as signatory for US DOE-signed GIF VHTR- Computational Methods Validation and Benchmark (CMVB) agreement and prepared for the spring meeting.
- Completed DataQuality081, a two-phase matrix test revisiting the depleted inventory state to examine a new method for inventory refill. The flow loop was operated until flow stagnation, at which point a high flow rate cold-refill method was initiated. The high flow, 20+ GPM, allowed replenishment of the system inventory without any stagnation-induced geysering events.
- Submitted a paper on depressurized conduction cooldown modeling and sensitivity studies for HTTF.
- Presented HTTF work at ANS Winter meeting.
- Transmitted a first draft of HTTF benchmark specifications to Organisation for Economic Co-operation and Development (OECD)-Nuclear Energy Agency (NEA) for their review.
- Working on best-estimate calculations for PG-29 and PG-27.

December

- Held a 1-day review meeting for the NSTF program team on December 13th, 2022, to present recently completed testing and simulation results, and then jointly discuss the path forward for the remaining water-based matrix testing. The final attendance included 25 meeting participants, six virtual and 19 in person. Represented at the meeting were federal, regulatory, and national labs (DOE, NRC, INL), four industry vendors (Framatome, X-energy, Kairos, and Boston Atomics), and two US universities (University of Wisconsin–Madison and Texas A&M University).
- Following conclusion of the meeting and in preparation for the extended holiday break and Laboratory shutdown, the experimental team placed the test facility into warm standby. Activities included draining all inventory from the test loop, powering off the high-voltage feed systems, enabling remote monitoring checks, and changing water filters in the storage tanks.

2. SIGNIFICANT ACCOMPLISHMENTS

2.1 Fuels Development and Qualification

2.1.1 Mesoscale Thermal-Transport Properties of As-Fabricated and Neutron-Irradiated TRISO Fuel Kernels and Particle Coatings

The thermal-transport properties of nuclear fuel influence fuel temperatures, and therefore fuel performance. Thermal-transport property measurements were performed at room temperature on as-received and neutron-irradiated TRISO fuel compacts as part of the AGR Fuel Development and Qualification Program. This work is the first time irradiated TRISO fuels have been subjected to thermal properties measurements. These initial exams were performed in the 4th Quarter of FY22, and the following are some preliminary results that were processed and analyzed from a few different samples in the 1st Quarter of FY23.

The irradiated samples used in these exams were cross-sections prepared from AGR-2 Compacts 5-1-3 and 2-4-3.[1] These compacts were irradiated at the Advanced Test Reactor (ATR) at INL, and Table 1 summarizes a few properties from that irradiation. The unirradiated samples were two particles that had been previously deconsolidated from an unirradiated compact that was fabricated as part of the AGR-2 experiment. These were previously prepared in mount LEU09-F52 for electron microscopy.

Table 1. Selected AGR-2 compact properties and mount identifiers.

Compact	TAVA[a] (°C)	Burnup[b] (% FIMA)	Fluence[c] (10^{25} n/m^2)	Mount
2-4-3	1216	11.52	3.08	58X
5-1-3	1078	11.09	3.03	64X

a. Time-average, volume-average irradiation temperature
b. Fissions per initial metal atom
c. Fast neutron fluence (E>0.18 MeV)

Mesoscale measurements were performed in the fuel kernels as well as in the fuel-particle coatings using thermal-conductivity microscopy (TCM). A thermal-conductivity microscope is an instrument developed at INL that uses a laser-based modulated thermoreflectance technique that uses an intensity-modulated laser beam (referred to as the "pump laser") to heat the sample and generate thermal waves that diffuse into the bulk of the sample. A second laser beam (referred to as the "probe" laser) is scanned across the heated region of the sample. Changes in optical reflectivity due to laser-induced heating of the sample are recorded at the pump-modulation frequency using lock-in detection. The relative phase of the probe beam as it is scanned across the spot heated by the pump beam is fitted to a three-dimensional (3D) thermal-diffusion model to extract the thermal diffusivity of the measured region. To facilitate high sensitivity, the polished TRISO compact cross-sections were coated with a thin (~80-nm-thick) gold film using a magnetron sputter coater. Gold was selected for its high thermoreflectance coefficient. Figure 1(a) shows an image of the TCM located inside the Thermal Properties Cell at the Irradiated Materials Characterization Laboratory (IMCL), along with a schematic of the laser-beam paths in the instrument. An optical image of the sample of an irradiated TRISO fuel particle is shown in Figure 1(b). The laser beams—focused to ~2-µm-diameter spots using a 50× microscope objective lens—are seen during a measurement inside an irradiated fuel kernel in the bottom image.

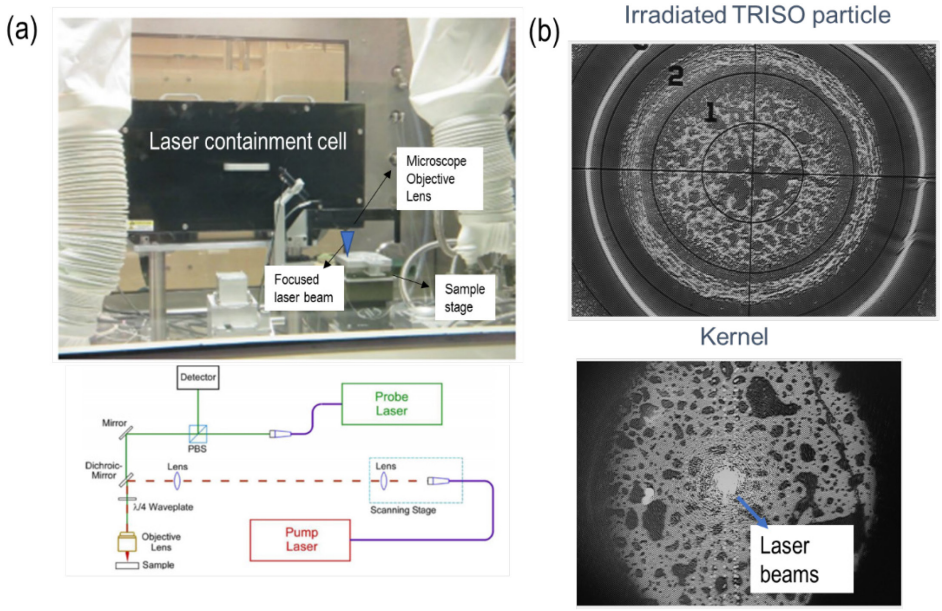

Figure 1. (a) Image of the TCM and (b) optical images of an irradiated TRISO fuel particle during measurement.

Mesoscale measurements were performed in the uranium oxycarbide (UCO) fuel kernel, the buffer layer, the inner and outer pyrolytic carbon layers (IPyC and OPyC, respectively), and the silicon-carbide (SiC) layer. Two particles from each of the compact cross sections were probed. Changing the laser beams' scan directions enables the measurement of thermal diffusivity along radial as well as circumferential directions. Baseline measurements were performed on the kernel and particle coatings of two as-fabricated TRISO particles (Mount LEU09-F52). Challenges in analyzing the signal from the SiC layer were encountered, and results are not reported here. The average values of the thermal diffusivities measured on the as-fabricated sample are listed in Table 2, along with some measurement from a surrogate TRISO particle examined in another study.

Table 2. Values of thermal diffusivity extracted from the laser-based measurements in different regions of an as-fabricated TRISO particle.

Sample region	Measurements on LEU09-F52 (mm2/s)		Measurements by Wang et al (2022) on a TRISO surrogate (mm2/s)[2]
	Radial	Circumferential	Direction not given in paper
Fuel	2.98	2.97	—
Buffer	5.38	5.05	4.05
IPyC	7.70	8.25	6.1
OPyC	9.42	10.21	3.95

We compare our measurements of thermal diffusivity to those reported by Wang and coworkers[2] on a surrogate TRISO sample using a similar technique. We see from Table 2 that although the thermal diffusivity values within the buffer and IPyC layers are within ~35%, there is a notable discrepancy between our measured values and those reported by Wang. Fluidized-bed chemical vapor deposition (FBCVD) process parameters, such as deposition temperature, coating-gas fraction, and gas-flow rate are known to affect the microstructure and resulting thermal properties of the layers.[3,4] We therefore attribute these differences between our findings and those reported by Wang to variations in the manufacturing process of the TRISO samples. We also note that while the fuel kernel and buffer layers are thermally isotropic, the IPyC and OPyC regions have a consistently higher thermal diffusivity along the circumferential direction when compared to the radial direction.

Figure 2 shows a bar chart that summarizes the measured thermal diffusivities of the as-received sample (shown in grey) along with the two irradiated compacts 2-4-3 (58X) and 5-1-3 (64X) shown in yellow and blue respectively. A reduction of up to 57.2% in the thermal diffusivity of the fuel kernel is observed following neutron irradiation. The values of thermal diffusivity of the fuel kernels of particles 58X and 64X are within ~6% of each other, despite being irradiated at different temperatures. A similar reduction in thermal diffusivity is also observed in the buffer layer following neutron irradiation. The preliminary analysis also indicates an increase in the thermal diffusivity of the pyrolytic carbon layers (ranging from about 15% in 64X to ~114% for 58X for the IPyC, and ~83% in 64X and ~58% for 58X for the OPyC regions). A thorough analysis of the measurements in the pyrolytic carbon layers is underway to determine if the thermal model fitting is affected by thermal transport in the adjacent layers. Our measurements are expected to inform the TRISO community on the reasonableness of thermal properties used in fuel performance modeling and to assess the evolution of thermal diffusivity with neutron irradiation.

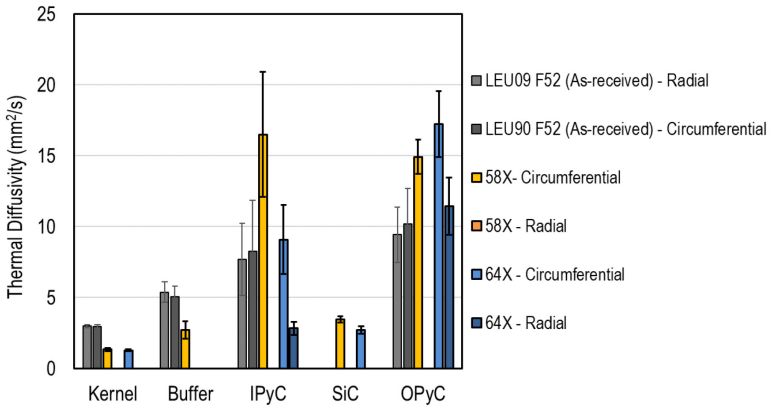

Figure 2. Measured thermal diffusivity of various regions within as-received and irradiated TRISO fuel particles along the radial and circumferential directions. Compact 2-4-3 corresponds to mount 58X and 5-1-3 corresponds to 64X.

For more information, contact:

John D. Stempien (john.stempien@inl.gov)

2.1.2 Generation IV International Forum Collaborations

AGR program staff from INL and ORNL attended the 18th official meeting of the GIF, VHTR Fuel and Fuel Cycle (FFC) Project Management Board (PMB) on October 18, 2022, in Cadarache, France. Staff also attended the 6th Workshop on Material Properties of TRISO Fuels the was organized in conjunction with the PMB meeting and held on October 19–20 in Aix-en-Provence, France.

The PMB meeting included a presentation by FFC PMB chair Paul Demkowicz (INL), updating the PMB members on TRISO fuel development- and performance-evaluation progress in the US. Other participants at the meeting included representatives from PMB member states China, France, and Korea, as well as PMB observers from Canada and the UK. In addition, John Hunn (ORNL) presented a summary of the current status of the ongoing LBL collaborative round-robin activities, which included plans to compile results from the participating PMB members (China, Korea, and the US).

The technical program for the workshop on TRISO fuel properties was organized by AGR program staff (Tyler Gerczak, ORNL) and included 24 presentations from five different countries and nine different institutions. Presentation topics included thermal-property measurements, pyrocarbon microstructure-property relationships, buffer and SiC microstructure and irradiation behavior, TRISO particle modeling and simulation, fission-product transport in TRISO particles, and unconventional TRISO fuels. This was the latest in a series of workshops hosted by the FFC PMB that started with a focus on SiC properties, but has since expanded to a much broader scope based on interest and research directions in the TRISO community in recent years. In addition to the many good presentations by participants, the workshop provided an excellent forum for technical discussions among the attendees on current topics of interest to the TRISO fuel community. On October 21, Commissariat à l'énergie atomique et aux énergies alternatives (the French Alternative Energies and Atomic Energy Commission) hosted a tour of the sites of the International Thermonuclear Experimental Reactor and the Jules Horowitz Reactor, both currently under construction at Cadarache.

For more information, contact:

Paul A. Demkowicz (paul.demkowicz@inl.gov)

John D. Hunn (hunnjd@ornl.gov)

Tyler J. Gerczak (gerczaktj@ornl.gov)

2.2 High-Temperature Materials

2.2.1 Development of New ASME Section III, Division 5, Design Rules for Class B Construction

The ASME BPVC, Section III, Division 5, High Temperature Reactors, provides the rules that govern the construction of vessels, piping, pumps, valves, supports, core-support structures and nonmetallic core components for use in high-temperature reactor systems and their support systems. Division 5 recognizes the different levels of importance associated with the function of each component as related to the safe operation of the high-temperature reactor plant. The code classes for metallic components, Classes A, B and SM, allow a choice of rules that provide a reasonable assurance of structural integrity and quality commensurate with the relative importance assigned to the individual components of the high-temperature reactor plant.

The current Class B rules are an extension of the low-temperature rules of Section III, Division 1, Subsection NCD, Class 2 vessel, pump, valve, and piping designs to elevated-temperature service. For temperatures in the creep regime, the Class B design rules are principally based on the design-by-rules provisions of ASME Section I and Section VIII, Division 1. These design-by-rules provisions do not cover the failure modes from cyclic service in the creep regime. Some overly conservative creep-fatigue rules were introduced for Class B piping to cover the gap.

The Class B rules do not employ the concept of variable design lifetimes for service loads. The allowable stresses in the creep regime for Class B components are based on the tabulated values in Section II, Part D, Tables 1A and 1B. These values are established by extrapolating creep and creep-rupture properties from shorter terms to 100,000 hours. Thus, the use of these allowable stresses for Class B components that have long (e.g., 500,000 hours) design lifetimes would be nonconservative.

To address these gaps, an effort was initiated in FY-22 to revamp the Class B design rules by introducing (i) design-by-analysis methods, (ii) ratcheting and creep-fatigue design provisions, and (iii) time-dependent allowable stresses, up to 500,000 hours, but with less-stringent data requirements. Guided by the more-comprehensive rules for Class A components, initial new design-by-analysis rules were developed by Sham, Mahajan, and Wang (2022) for evaluating the primary load limit, strain limits and creep-fatigue damage of Class B components with variable lifetimes.[5] Due consideration was given to the reasonable assurance of structural integrity and quality commensurate with Class B components in developing these new rules. The technical basis of the new Class B rules is shown in Table 3.

Table 3. Technical basis for the new Class B design-by-analysis rules.

New Class B Design-by-Analysis Rules	Technical Basis
Primary load limit	Global limit load check from Class A elastic perfect-plastic (EPP) primary load code case (no local check)
Strain limits	Requiring only plastic shakedown from the Class A EPP strain limits code case (no checks on equivalent strain at interior points)
Creep-fatigue damage	Elastic analysis results from Class A elastic creep-fatigue procedure, with creep damage calculated using the isochronous stress-strain curves, but along a follow-up modified stress relaxation path

In the reporting period, the new Class B rules were assessed using the Alloy 617 p-SMT test results developed at the ORNL (Wang et al. [2019]).[6,7] Figure 3 shows the Alloy 617 p-SMT test specimen which is loaded at elevated temperatures by cyclic displacement at the ends and constant pressure internally. Figure 4. shows the finite element modeling of the Alloy 617 p-SMT test specimen.

Figure 3. Alloy 617 p-SMT test specimen, photo by ORNL.

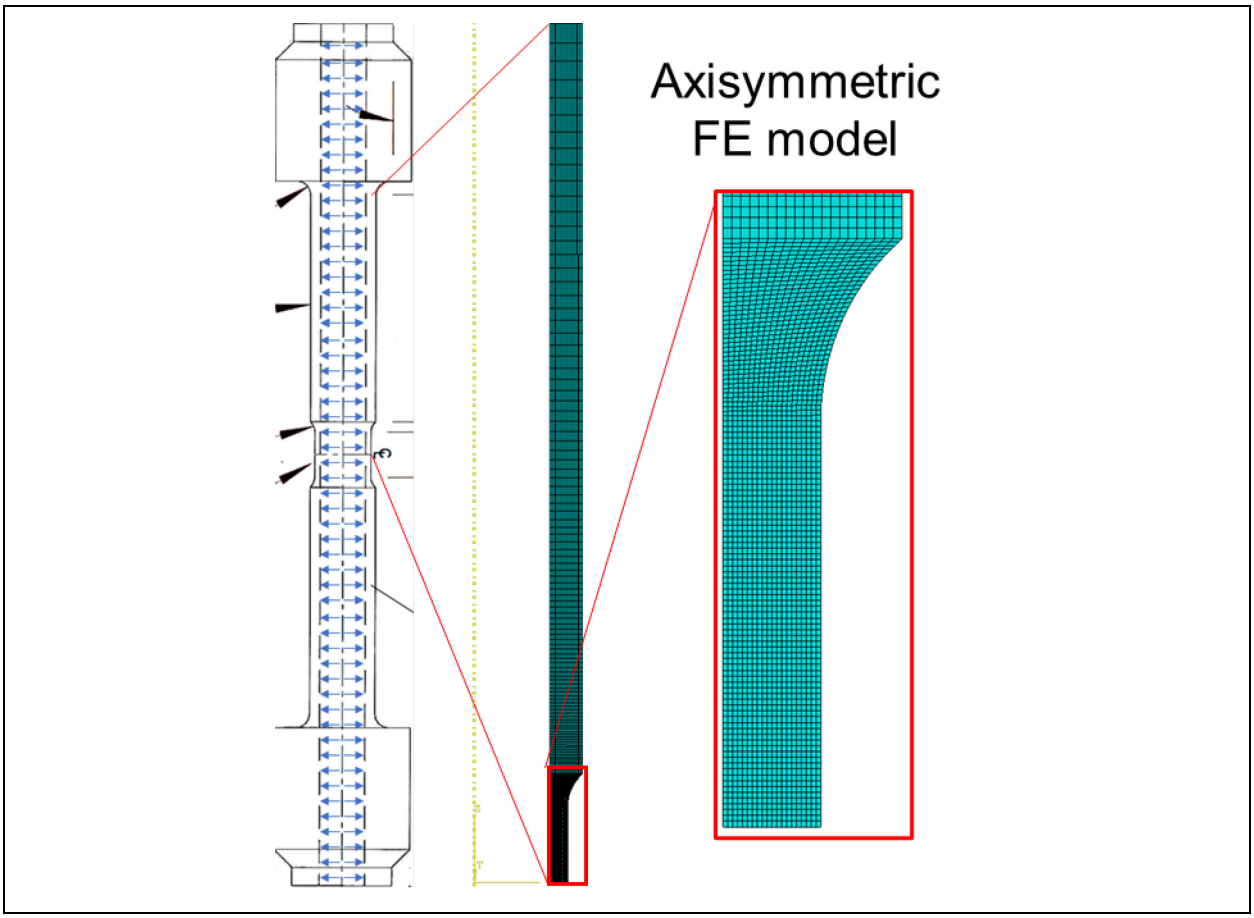

Figure 4. Finite element model of the Alloy 617 p-SMT test specimen.

Six test conditions for the Alloy 617 p-SMT testing conducted at the ORNL were selected for assessing the new Class B creep-fatigue evaluation procedure. The Alloy 617 p-SMT test conditions and the corresponding cycles-to-failure results are shown in Table 4 under the Experimental Results heading. Class A elastic analysis method, Class A inelastic analysis method, and the new Class B creep-fatigue analysis method were applied to the six test conditions to predict the corresponding maximum allowable design cycles. These predictions are shown in Table 4 under the Analysis Results heading. All analysis methods gave predictions more conservative than the experimental results. The new Class B creep-fatigue analysis method with an elastic follow-up factor (q) of 3, predicts higher maximum-allowable design cycles than is permissible under the more conservative Class A elastic analysis method. The predictions from the new Class B creep-fatigue analysis method are more conservative than the more-accurate Class A inelastic analysis method. Thus, the predictions from the new Class B creep-fatigue evaluation procedure follow the expected trend for the Alloy 617 p-SMT configuration. We will use a more prototypical sample problem—e.g., a flat-head vessel—to assess the new Class B rules in the next quarterly report.

Table 4. Comparison of experimental results against predictions from different design rules.

Experimental Results							Analysis Results			
			Hold Time (sec)				Maximum allowable design cycles***			
ID	Test Temperature (°C)	End Displacement ± δ(mm)	Tensile hold	Compressive hold	Pressure (MPa)	Cycles to failure from test	Class A Elastic (K'=0.9)	Class A Inelastic Analysis**	Class B [K'=1] (q=1)	Class B [K'=1] (q=3)
P01	950	0.1143	600	0	0.01	220	10*	49	37	16
P05	950	0.1143	600	600	0.01	320	8*	35	32	14
P02	950	0.1143	600	0	1.38	220	10*	49	37	16
P12	950	0.0635	600	0	0.01	1360	29*	218	90	38
P14	850	0.0762	600	0	2.76	3440	87*	364	336	115
P15	850	0.0762	600	0	0.14	3460	97*	368	336	115

* These p-SMT tests did not satisfy the Appendix HBB-T Tests A1, A2, A3 (XIII-3420), B1 and B2 for the ratcheting check using Class A rules. Only Test B3 was satisfied.

** Class A inelastic analysis results by Barua et al (2021). [8]

*** For Class A elastic and Class B analysis procedure, maximum allowable design cycles are calculated based on their respective creep-fatigue damage envelope

2.2.2 Inelastic Constitutive Models for ASME Section III, Division 5 Materials

Recent work in the Gas-Cooled Reactor High-Temperature Materials area has established a new Nonmandatory Appendix Z to Section III, Division 5, of the ASME BPVC that provides constitutive models for use with the Section III, Division 5, Class A design by inelastic analysis rules. These models promote the use of the more-accurate design by inelastic analysis methods by relieving the designer or owner/operator from the burden of developing and validating a constitutive model themselves. Models for four materials—Grade 91 steel, 316H stainless steel, the nickel-based Alloy 617, and the nickel-iron-chromium Alloy 800H—have either been approved or are under consideration at the cognizant ASME Code Committees.

All four models have significantly different mathematical forms. While differences in material behavior may justify or require treating each material with a bespoke model, the mathematical exposition and detailed explanation required to describe and document the models in the Code are significant logistical challenges. The challenge carries over to implementing the models for use in design calculations, as the computer implementations of the models are likewise significantly different.

A task has been initiated to explore the feasibility of a universal high-temperature inelastic constitutive model, general enough to accurately capture the key material behaviors of these four materials. Should such a model exist, it would greatly simplify the new Appendix Z and further reduce the investment required by designers to apply the design by inelastic analysis rules.

In the reporting period, efforts were made to define a generalized constitutive model, and to fit the model form for the four materials using the test data collected as part of the effort to develop the original constitutive models. As an initial step, only monotonic deformation data from tensile and creep tests are used to calibrate the models for each material. The one-dimensional (1-D) generalized model form selected for this initial consideration was that of a Chaboche/Perzyna viscoplastic model based on overstress. Voce hardening and static recovery were used for the evolution of the isotropic hardening parameter.

Deterministic and statistical models were constructed from the generalized constitutive model for data fitting, or data training, of the four materials listed above. The statistical approach can also quantify heat-to-heat variability in the material response, as described by Messner (2022).[9] Typical comparisons of the predictions from the models and test data are shown in Figure 5. for Alloy 800H tensile tests, with (a) from the deterministic model, and (b) from the statistical model.

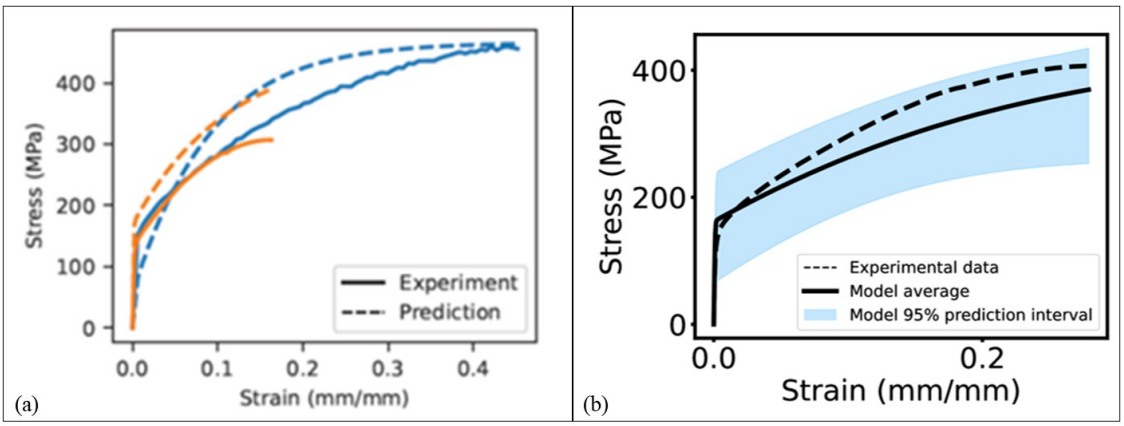

Figure 5. Comparison of model predictions to Alloy 800H tensile data, (a) deterministic model, (b) statistical model.

The preliminary results indicate that the use of a generalized constitutive model form to describe the deformation behaviors of the four Division 5 Class A materials is promising. The next step is to develop an approach to adequately describe the temperature dependence of the model parameters, particularly for temperature range where test data are scarce. This will be followed by the extension of this "universal" constitutive model approach to the more complex cyclic deformation behaviors.

For more information, contact:

Sam Sham (tingleung.sham@inl.gov)

2.3 Graphite Development and Qualification

2.3.1 AGC-4 Experiment

Non-destructive analysis of one of the high-activity AGC-4 samples was performed using two techniques. The first was X-ray fluorescence (XRF), and the second, combined laser-induced breakdown spectroscopy (LIBS)/time-of-flight (TOF) mass spectroscopy. The first is useful for general-area metals identification while the second allows mass-specific identification. The item analyzed was AGC-4 CAN114 (Figure 6.), which contains a highly oriented pyrolytic graphite sample inside a 12.7-mm-diameter × 12.7-mm-high graphite container. The sample was located in the center channel, approximately at mid-level in the experiment. Preliminary data from TOF and LIBS analyses are shown in Figure 7 and Figure 8.

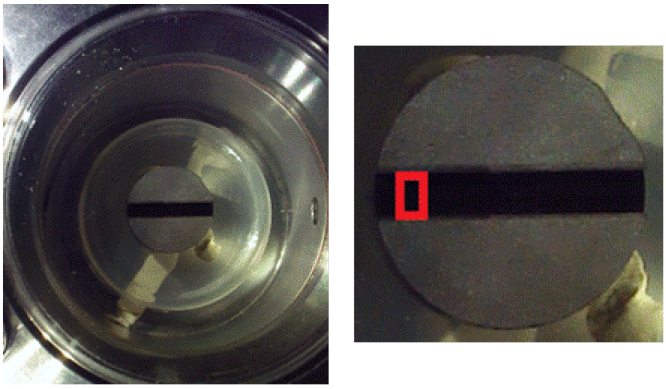

Figure 6. AGC-4 CAN114, which contains a highly oriented pyrolytic graphite sample inside a 12.7-mm-diameter × 12.7-mm-high graphite container.

The XRF showed the presence of copper and manganese, as well as calcium. A standard for these elements may need to be acquired to provide confirmation of the detection. The multiple data points across the face of the can, measured by LIBS/TOF, confirmed the presence of copper, nickel, and iron. The multipoint scan indicated some variation from edge to edge of the container face, but had consistent detection of several metals. Quantitative confirmation on the concentrations and elements is in process. Additional scans of the can are planned to determine whether the first indications are consistent over the container surface. Previous measurements of the container using gamma-ray spectroscopy indicated the presence of cobalt-60, which is assumed to be the main contributor to the higher-than-expected dose rate experiment.

Another of the high-activity samples, DA4809, a piggyback sample made of PCEA graphite was measured as having 750 mR/hr beta-gamma at contact. It was measured with gamma-ray spectrometry, and the prevailing nuclide was identified as cobalt-60. Because this sample was too active for nominal contact handling, the item was placed in the AGR burnback furnace in MFC AL Hot Cell 5. A special quartz container was fabricated with a porous plate bottom that allowed air to be forced through to promote oxidation. The sample was oxidized over 24 hours at 750°C, resulting in a nearly undetectable amount of ash. The container was leached with nitric acid, and an aliquot of the solution was taken to be processed through a conventional mass spectrometer to determine what metals may have been present that may not be detectable by gamma spectrometry. Analysis has not been completed at this time.

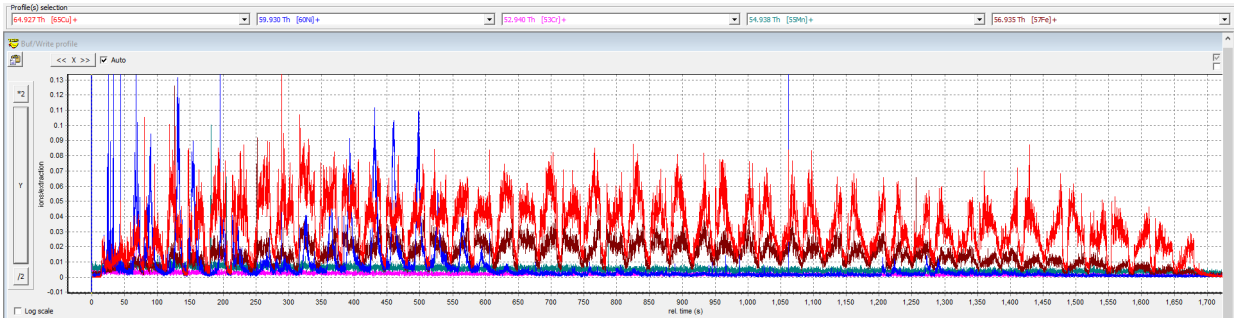

Figure 7. Preliminary TOF data for analysis of AGC-4 CAN114. Raw data (Cu, Ni, Cr, Mn, and Fe) indicates a couple of spots where Ni seems to be deposited.

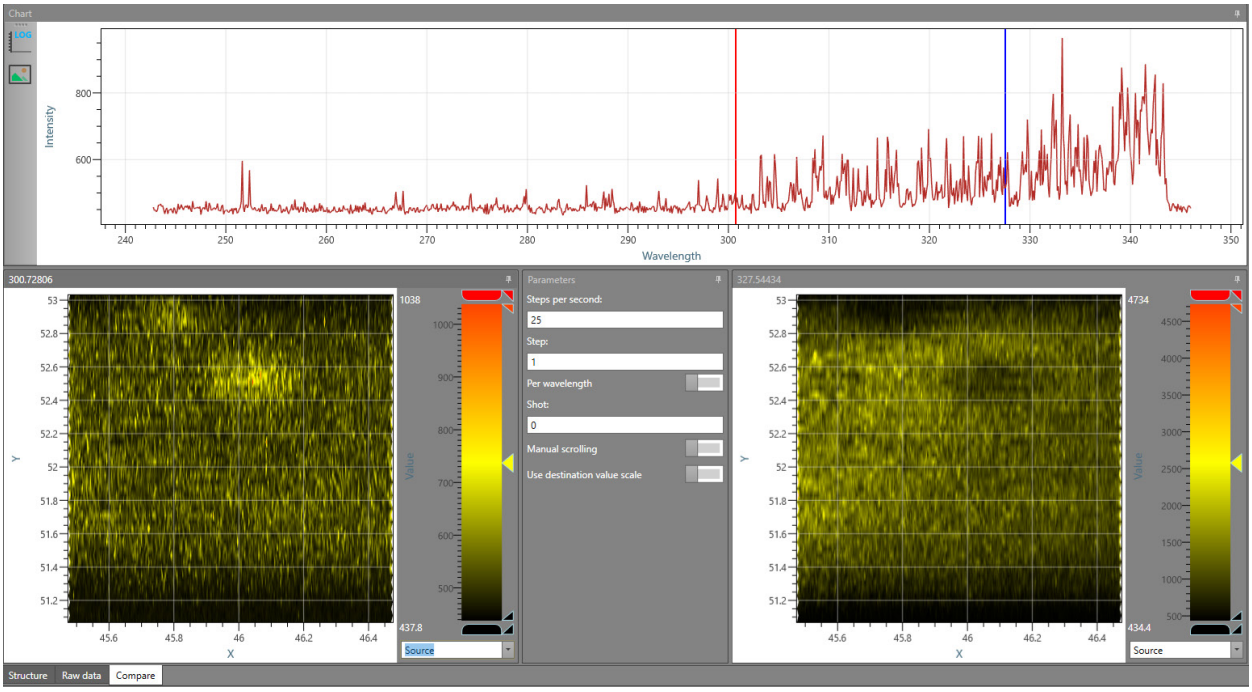

Figure 8. LIBS preliminary heat map for analysis of AGC-4 CAN114. The comparison of Ni and Cu shows a Ni hot spot where the Cu is less abundant.

2.3.2 Digital Image Correlation—Small Disc Compression Test of Graphite IG-110 with DIC Strain Measurement

Graphite grades Mersen 2114 and IG-110 are categorized as super-fine-grain graphite because they have a similar grain- and pore-size distribution; however, they are made from different raw materials and have distinct pore networks.[10,11] The 2114 graphite uses nonpetroleum coke and is formed with an isostatically molded method. Its average grain size is about 13 μm. IG-110 has a similar superfine grain size of about 20 μm, but its coke source is from petroleum and uses an isostatically pressed method in its forming process. Previous reporting shows that, although their mechanical behaviors are very similar, Mersen 2114 is slightly stronger than IG-110 in both tensile and compressive strength.[12]

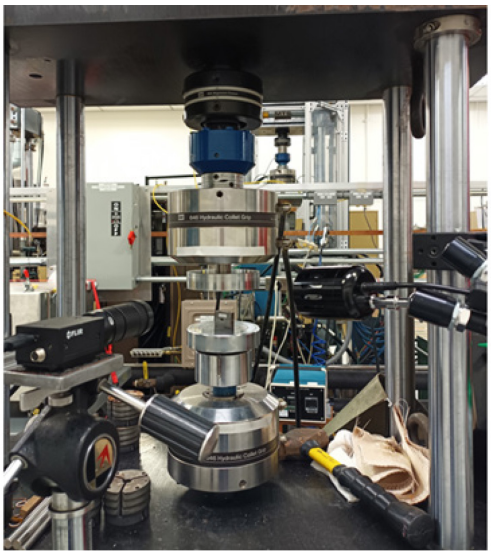

Figure 9.Hydraulic compression test frame used for compression testing of small specimens.

To continue our studies on combining digital image correlation while split disc testing following ASTM D8289,[14] 10 samples from graphite-grade IG-110 discs (Ø6 × 3 mm) were tested with the same test protocol and loading frame previously applied to samples of Mersen 2114. The hydraulic machine used for disc compression tests is shown in Figure 9. All 10 discs were compression tested until the sample cracked. Photos of samples are shown in Figure 10.

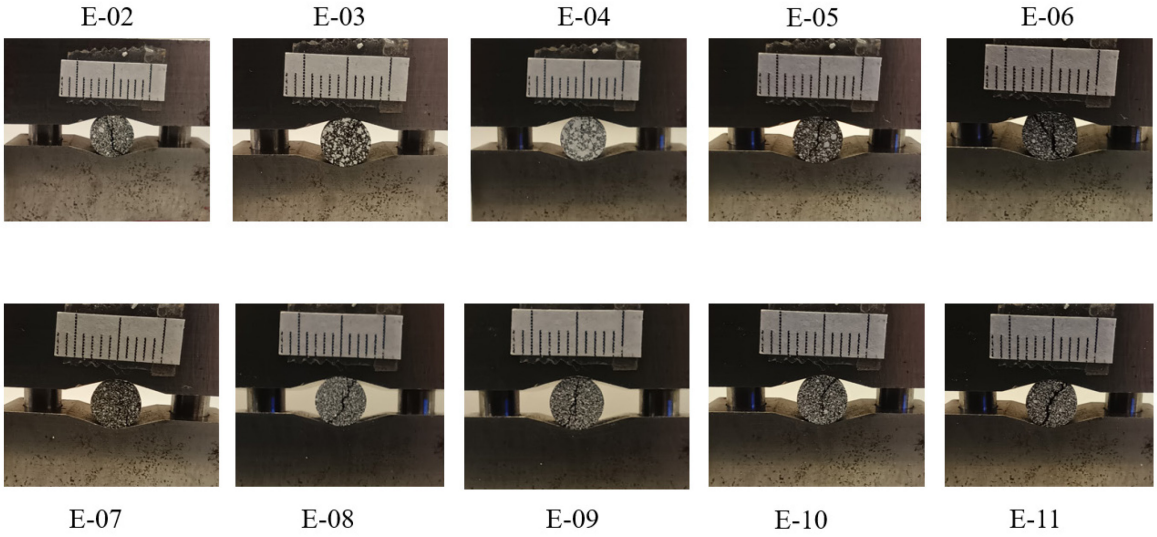

Figure 10. Cracked samples, white dots are painted for digital-image-correlation measurement.

The splitting tensile strength, σ_{sts} (MPa), of the graphite samples can be calculated from Equation (1)[13]:

$$\sigma_{sts} = 0.931\ P/(\pi LR) \quad (1)$$

where

P = maximum applied load (N)

L = specimen thickness (3 mm)

R = specimen radius (3 mm).

The maximum applied load recorded for these 10 samples, along with the calculated splitting tensile strength (Eq. (1)), are listed in Table 5. The average splitting tensile strength of these 10 IG-110 samples is 29.23 MPa, with a standard deviation of 4.89 MPa.

Table 5. Peak load of 10 samples of IG-110 in splitting disc test.

Specimen	Peak load (N)	σ_{sts} (MPa)
E-02	1218	40.1
E-03	1000	32.9
E-04	975	32.1
E-05	895	29.5
E-06	877	28.9
E-07	856	28.2
E-08	832	27.4
E-09	733	24.1
E-10	758	25.0
E-11	732	24.1

Figure 11 shows results for two tests, samples E-02 and E-05 to illustrate the typical load and displacement curves recorded from loading machine. The blue displacement curve keeps linearly increasing with time due to the stroke-control mode setting in the machine and drops immediately when the test terminates. However, as highlighted in the orange load curves, roughly two different stages can be observed from the time-load history. The loading force increases with a slower slope at the beginning (before ~30–40 seconds for E-02 and E-05 samples), then grows faster at the second stage before reaching the failure point. The sudden drop of load curve indicates the disc cracks, and the maximum load is recorded before this failure point.

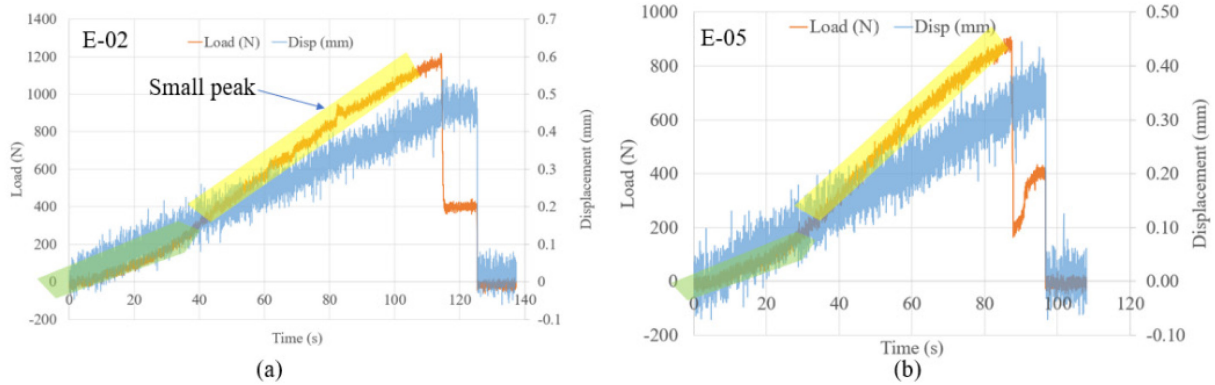

Figure 11 Load and displacement curves of splitting disc compression test on graphite IG-110, (a) E-02 sample, and (b) E-05 sample.

With digital-image-correlation device integrated in the compression test, more in-plane strain distribution on the disc surface can be extracted through the test. Taking sample E-08 as an example, Figure 12 shows the strains and their distribution before and after the crack appears. Strains at the center crack are difficult to calculate due to the generation of new geometric features and the loss of pixel tracking in that local region, so they have empty values around the crack, as shown in Figure 12d, e, and f.

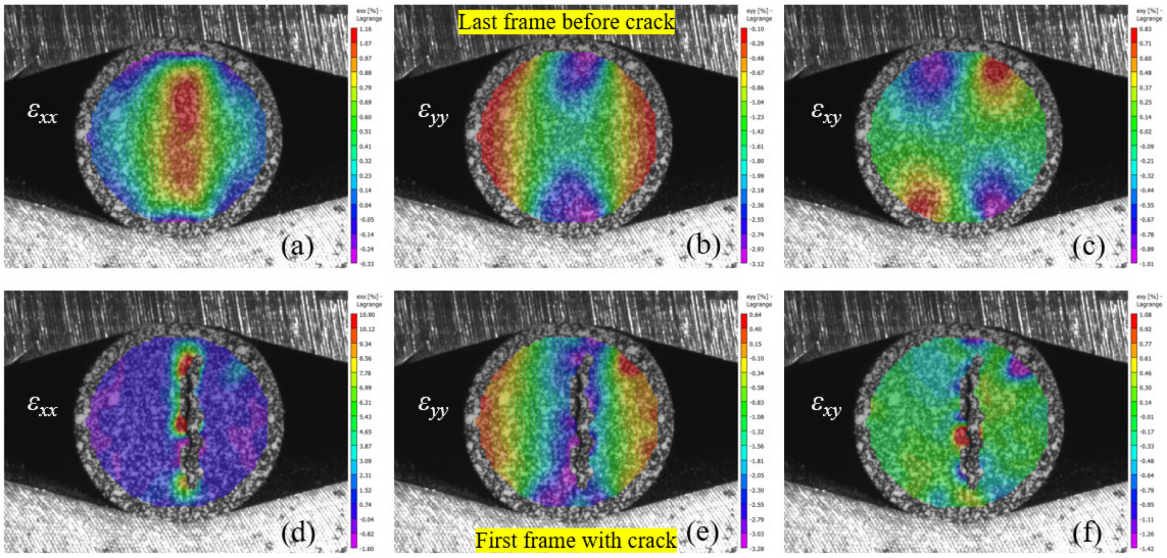

Figure 12. Strains extracted from digital-image-correlation system for sample E-08. Top row for strains of the last image frame before crack, and bottom row for the first image frame with crack. (a), (d) Strains in horizontal direction, e_{xx}; (b) (e) Strains in vertical direction, e_{yy}; (c) (f) Strains in shear, e_{xy}.

To understand the strain history near the disc center region, a square block was selected in that area to extract strain data. The extracted strain history of the selected 17 × 17 pixels center block is plotted in Figure 13 the green curves represent the values at the center point of the selected block, and red curves represent the averaged values in the selected block. The horizontal tensile strain ε_{xx} (Figure 13a) experienced several strain bumps before the appearance of the major through-center crack. The same small bumps were observed in the vertical compressive strain ε_{yy} (Figure 13b). The green averaged strains are used in the following calculation to represent the strain level at disc center due to the limited space resolution from the lens on such a small sample.

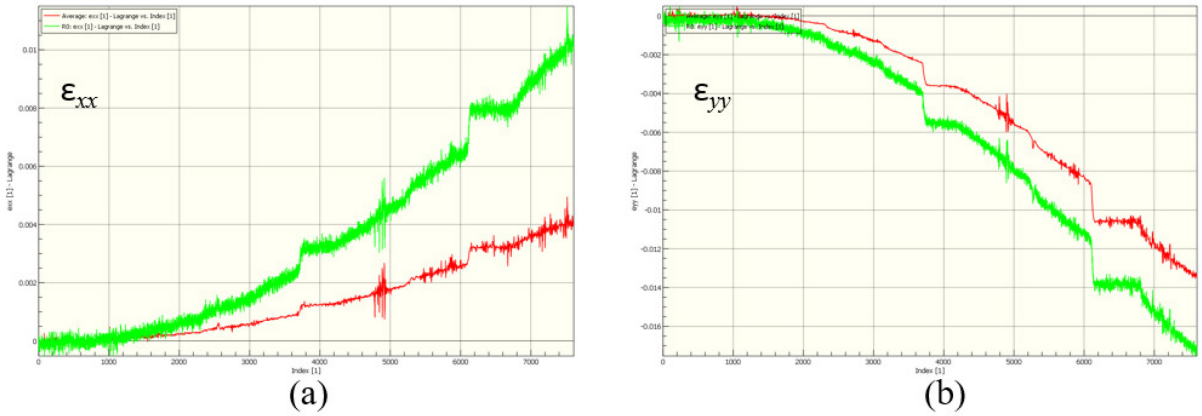

Figure 13. Strains extracted from E-08 disc center block, green for center point value and red for average block value, a) horizontal strain, b) vertical strain.

More details of the strains calculated in analytical solution and finite-element simulation, along with the results comparison between Merson 2114 samples and IG-110 samples, will be reported in next month.

2.3.3 Microstructural Studies

2.3.3.1 Microstructural Changes with Temperature

A manuscript was published:

S. Johns, T. Yoder, K. Chinnathambi, R. Ubic, W.E. Windes, "Microstructural changes in nuclear graphite induced by thermal annealing," *Materials Characterization*, 194 (2022) 112423. https://doi.org/10.1016/j.matchar.2022.112423. In this study, virgin nuclear graphite IG-110 was annealed at 2500°C to observe any microstructural changes due solely to high-temperature thermal annealing. The results shown in this study suggest that fullerene-like defects (Figure 14a–d), which are not observed in as-prepared nuclear graphites, will arise due to thermal annealing near graphitization temperature. Consequently, such defects may directly contribute to non-recoverable physical property changes previously observed in irradiated nuclear graphites.

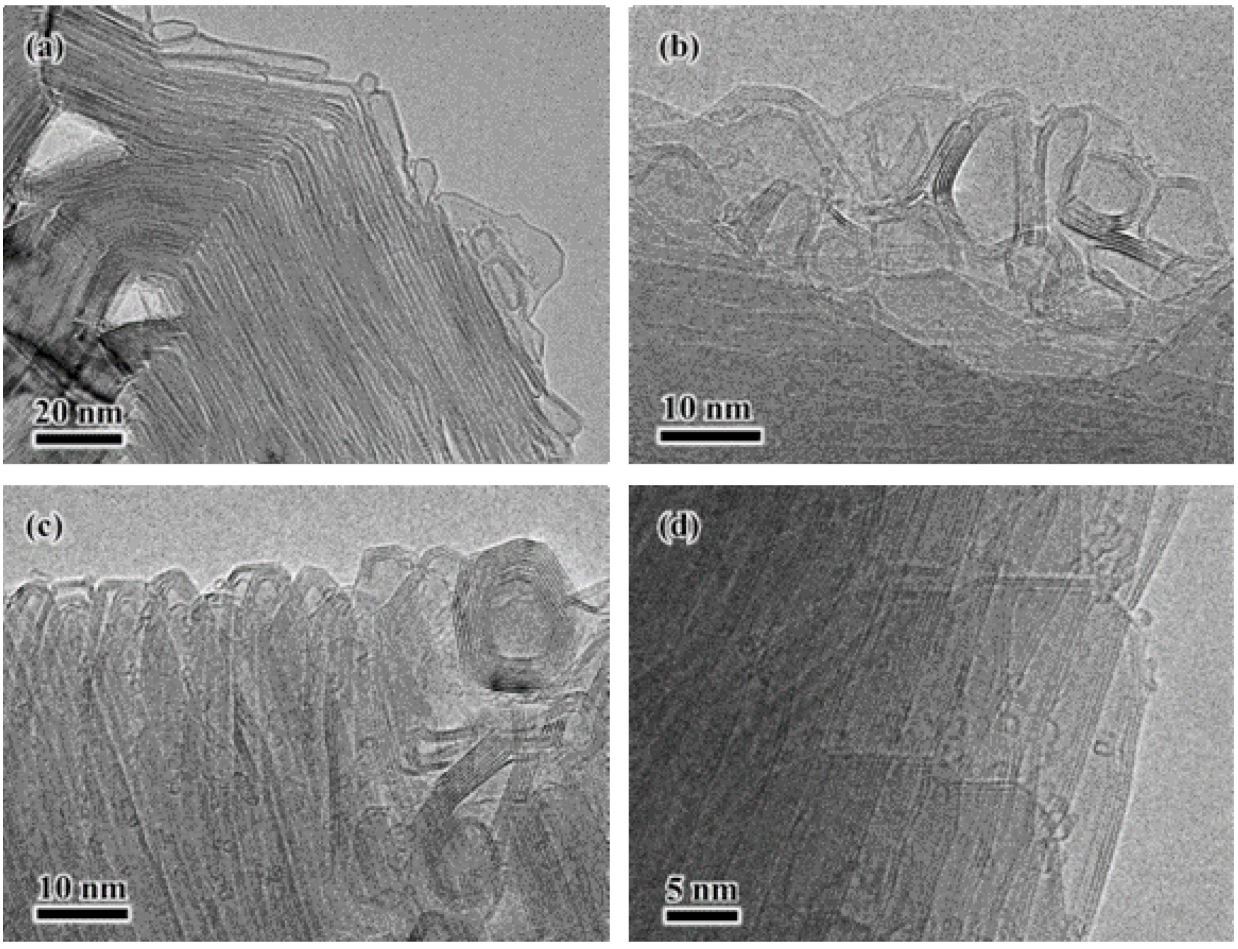

Figure 14. HR TEM micrographs of annealed IG-110. (a) shows the edge of the annealed specimen where fullerene-like structures are abundant. (b) shows further evidence of a poorly graphitized phase. (c) shows the edge of a crystallite oriented perpendicular to the c-axis where all basal plane edges have rearranged into faceted closed structures. (d) shows a crystallite decorated with small fullerene structures.

Additionally, a full-length paper, entitled "Semi-empirical modeling of irradiation-induced dimensional change in nuclear graphite H-451," has been accepted for *Proceedings of the ASME 2023 Pressure Vessels & Piping Conference* (yet to be published). In this work, historic data for nuclear graphite H-451 is revisited. A semi-empirical methodology is proposed to describe the dimensional change behavior as a function of temperature for nuclear graphite H-451. The turnaround dose, or when there is a reversal of the dimensional change from contraction to expansion, is proposed to be a thermally activated process; thus, it can be described by an Arrhenius model.

Specifically, for ASME code development, the methodology mentioned above is proposed by the authors to be modified for a universal activation energy for all nuclear graphites. The hypothesis is that all nuclear graphites are the same on the atomic level, containing sp2-bonded carbon with some degree of disorder. Thus, the pre-exponential can be used to describe the macroscale properties of a grade of nuclear graphite. These properties include grain size, anisotropy, and density. To normalize the analysis to include all grades of nuclear graphite, as opposed to the linear dimensional change, volumetric dimensional change normalizes the graphite billet's geometry. The preliminary results are shown in Figure 15 in which the developed model fits irradiation data with an R2 value of 0.99995.

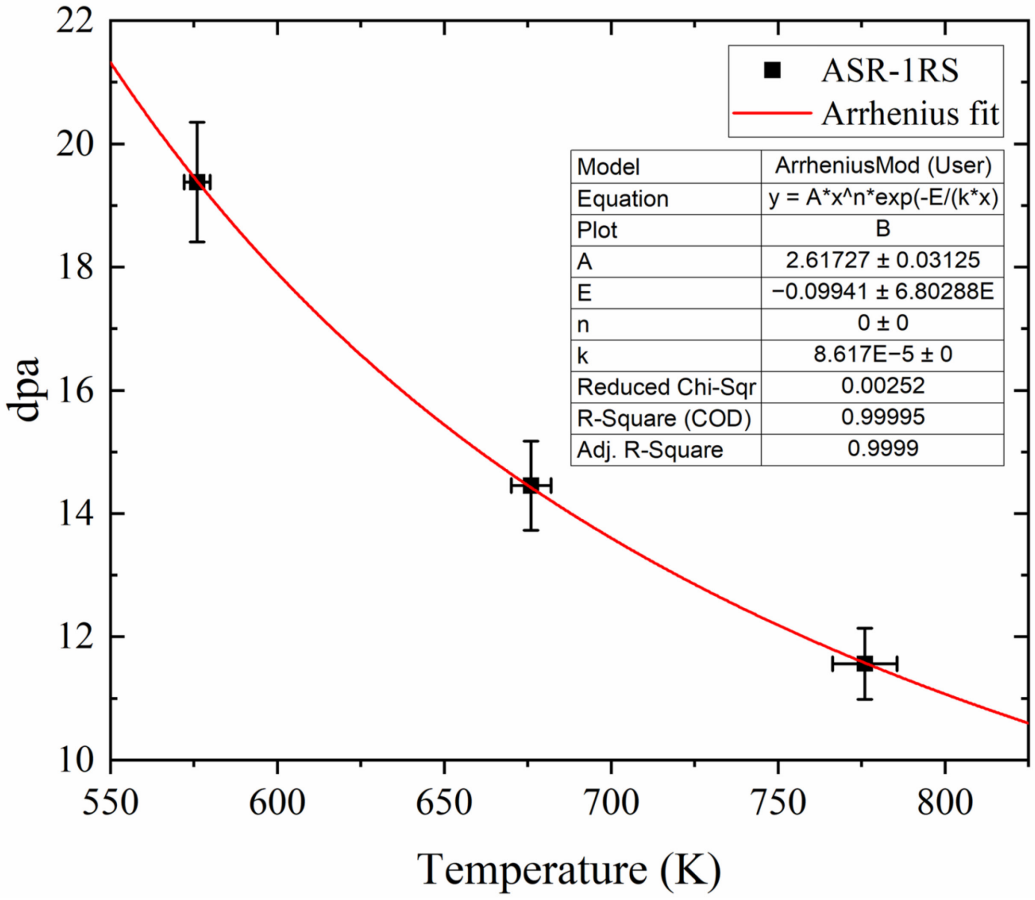

Figure 15 Modified-dimensional-strain methodology, assuming a universal activation energy, to describe volumetric-turnaround behavior in nuclear graphite ASR-1RS.

2.3.3.2 *Microstructural Characterization of the Oxidation of Nuclear Graphite under Accident Conditions via Synchrotron XCT*

Oxidation can be one of the limiting factors of a nuclear-graphite core because this degradation mechanism can reduce mechanical properties and neutron-moderation capacity. Graphite oxidation can occur under normal nuclear-power-plant operation due to the contact of impurities in the coolant or during the accidental ingress of air into the core. During an accidental ingress of air into the core, the air would react vigorously with graphite components, oxidizing the exposed surfaces. Synchrotron XCT was used to characterize the effects of oxidation under accident conditions on three nuclear grades IG-110, NBG-18, and PCEA. Synchrotron XCT offered the high temporal and spatial resolution required for this experiment. A furnace designed to operate on the I13 Diamond Light Source allowed for reaching the 700–750°C range used to simulate accident conditions. The furnace has multiple cavities that allowed continuous scanning via synchrotron XCT and access to air (Figure 16).

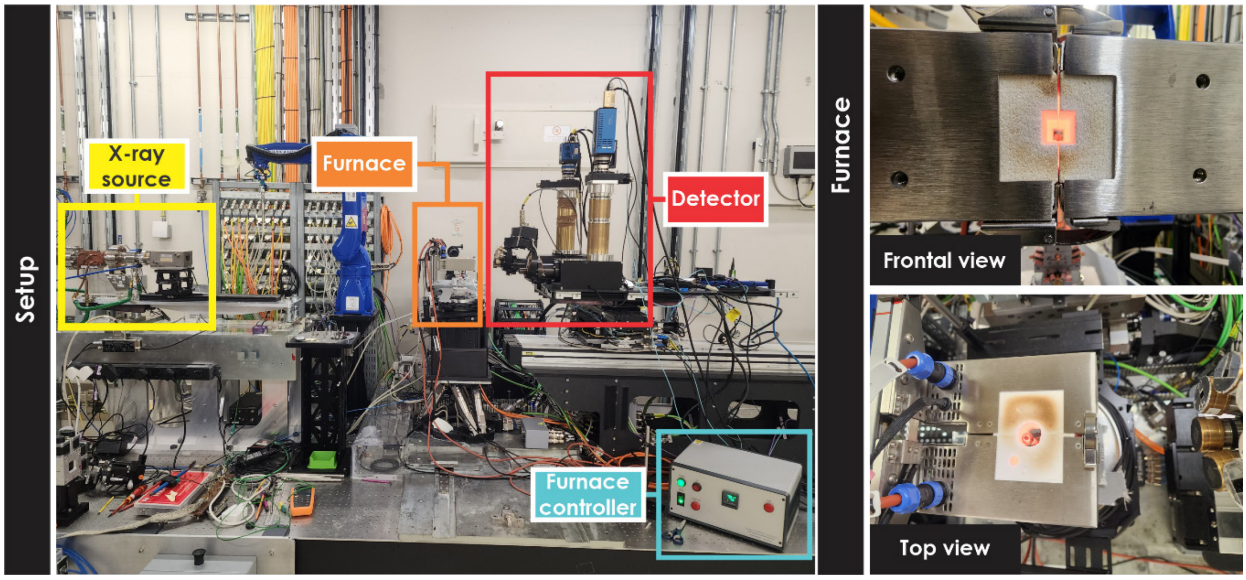

Figure 16. Setup at I13 and furnaces use for the oxidation experiments.

Preliminary results in Figure 17 show the removal of material and porosity generation at the top surface of an IG-110 specimen after about 90 minutes of oxidation at ~700°C. The ORNL and University of Manchester graphite groups performed these experiments. The ORNL team is working on segmenting and processing the XCT scans to produce a journal publication.

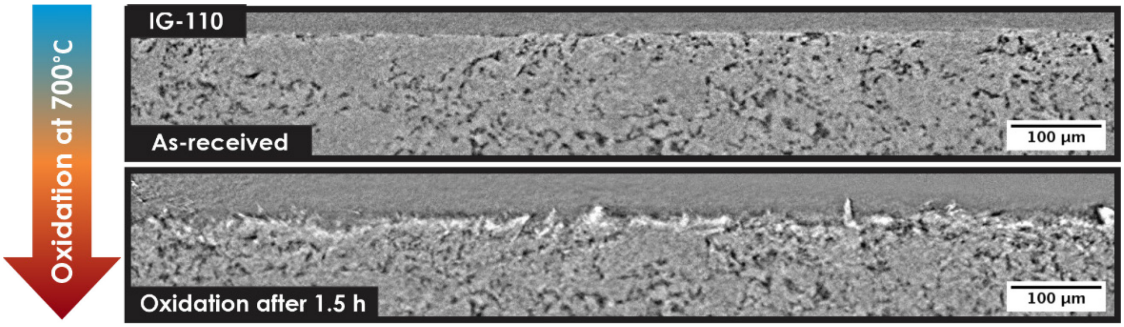

Figure 17. Preliminary synchrotron XCT oxidation results of IG-110.

2.3.3.3 Intra-grade Density Variations of Graphite Grade PCEA

Helium pycnometry measurements were conducted on samples from two batches of PCEA to understand the intragrade variations in this grade of nuclear graphite. These measurements are part of the current efforts to create a robust library of microstructures of modern graphite grades that can quantify the differences between different grades and intragrade variations. The helium pycnometry measurements shown in Figure 18 indicate that the batch labeled PCEA-1 tends to have a lower density than PCEA-2. Helium pycnometry measurements appear to be sensitive enough to detect the density variation between these two batches of PCEA. Additional measurements are being conducted in another batch of PCEA. Additional microstructural analysis will be performed on some of the specimens to understand the porosity structure and morphology of the filler phase.

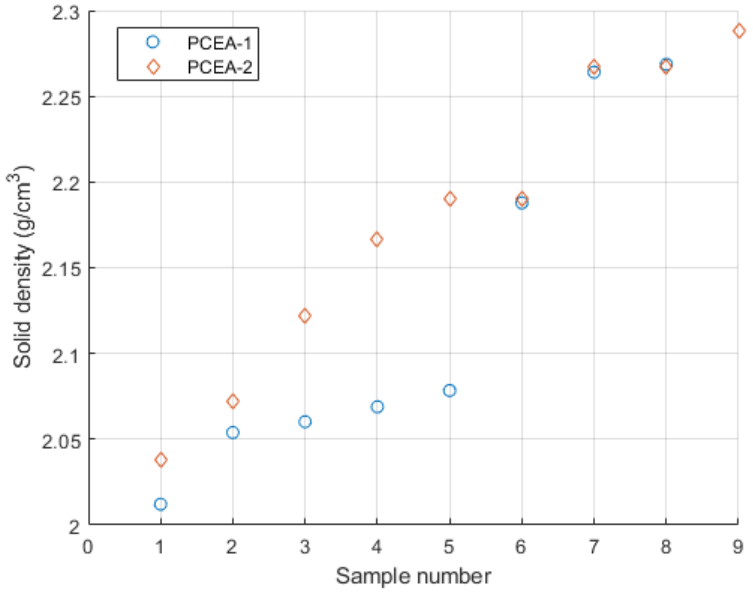

Figure 18. Solid density of PCEA-1 and PCEA-2 measured using helium pycnometry.

2.3.3.4 Graphite Lathing Studies

Work is currently underway to compare the density gradients among seven grades of graphite with oxidation to 2, 5, and 10% mass loss. Graphite grades include IG-110, NBG-18, IG-430, ET-10, ETU-10, 2114, and PCEA (Figure 19a-n). Initial samples are solid right cylinders machined to 2 inches in diameter by 1 inch tall. Samples are oxidized at 500°C to the prescribed mass loss and successively reweighed and remeasured as thin uniform layers (nominally 0.5 mm thick) are lathed from the entire circumference of the cylinder. The lathing methodology will demonstrate a benchmark for other, less-laborious approaches for the evaluation of the density profiles of oxidized graphite articles, such as optical analysis.

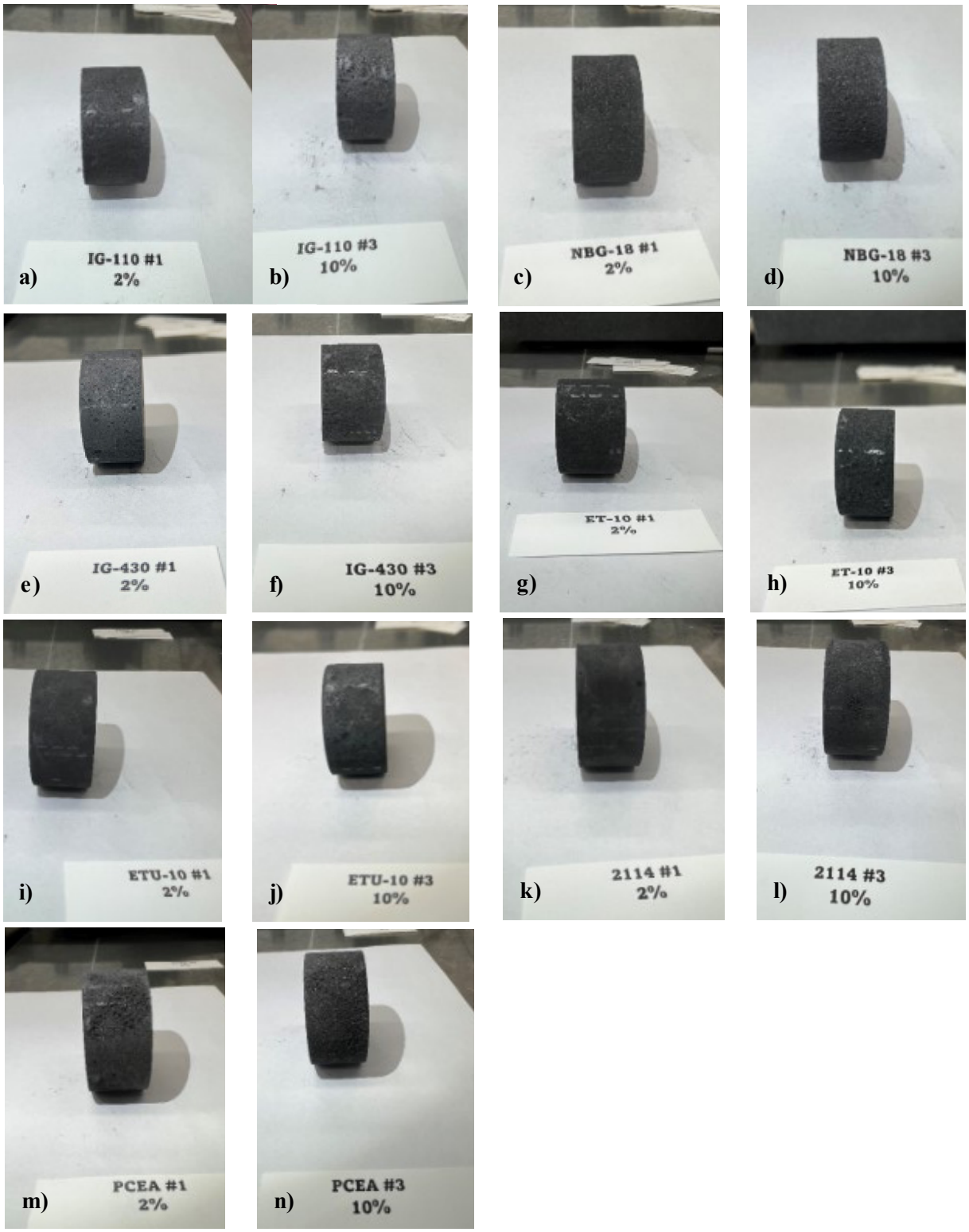

Figure 19. Examples of graphite specimens for lathing studies to compare density gradients with oxidation:(a) and (b) show IG-110 at 2% and 10% mass loss, (c) and (d) show NBG-18 at 2% and 10% mass loss, (e) and (f) show IG-430 at 2% and 10% mass loss, (g) and (h) show ET-10 at 2% and 10% mass loss, (i) and (j) show ETU-10 at 2% and 10% mass loss, (k) and (l) show grade 2114 at 2% and 10% mass loss, and (m) and (n) show PCEA at 2% and 10% mass loss.

2.3.4 Irradiated Graphite Oxidation Testing

Oxidation testing of both unirradiated and irradiated A3 matrix graphite has been completed for quartered piggyback specimens using a thermogravimetric analyzer (TGA) in the INL Carbon Characterization Lab. The irradiated A3 samples received doses between 6.3 and 6.55 dpa. The oxidation rate of irradiated A3 is almost the same as unirradiated A3, as illustrated in the Arrhenius plot in Figure 20. Contrary to the effect seen for NBG-25 graphite specimens tested (for a similar range of doses between 6.2 and 6.84 dpa), no acceleration of oxidation is observed to the A3 matrix graphite due to irradiation using the conventional rate analysis recommended in ASTM D7542, *Standard Test Method for Air Oxidation of Carbon and Graphite in the Kinetic Regime*.

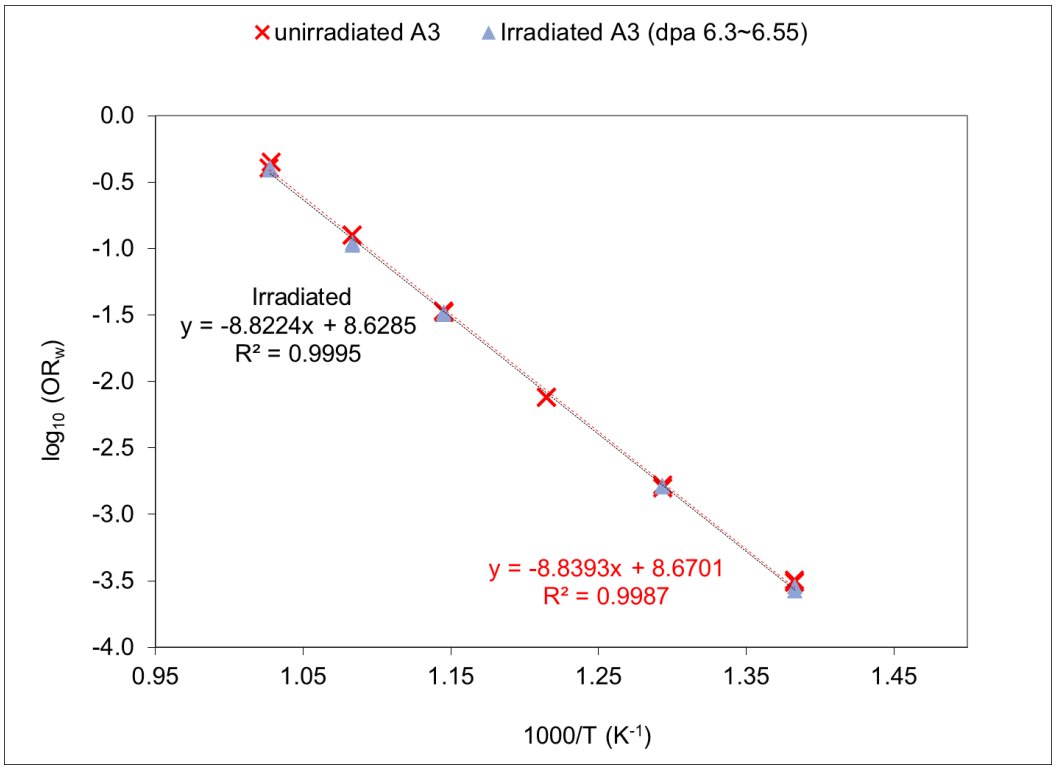

Figure 20. Arrhenius plots of oxidation rate data (normalized by initial mass) for irradiated and unirradiated A3 matrix graphite.

2.3.5 Vendor Irradiation Capsule Workshop

The first of two Vendor Irradiation Capsule Workshops was hosted at ORNL October 3–4, 2022. This workshop brought together more than 40 people to discuss the future needs for irradiation testing of graphite beyond the scope of the current Advanced Graphite Creep (AGC) program. Participants joined from national laboratories (ORNL, INL, UK's National Nuclear Laboratory), reactor designers (X-Energy, Kairos Power, Radiant Nuclear, FLiBe Energy, Westinghouse Electric, USNC, Framatome), graphite manufacturers (Ibiden/MWI, Mersen, SGL, Toyo Tanso, Tokai Carbon, Amsted Graphite Materials), the University of Manchester, nuclear consultancy firms Jacobs, and regulators from the US NRC.

The primary aim for this workshop was to bring together people with a wide range of vested interests in the data needs for graphite in support of those advanced nuclear reactors designed to use graphite as a neutron moderator. The workshop itself was meant to be a directed discussion about current reactor design needs above and beyond the data that are currently available or being created through the AGC program. It also intended to clarify how DOE's Office of Nuclear Energy will facilitate this effort going forward. DOE 's primary goal is to encourage the vested parties to work together in sharing costs and reactor space for future graphite-irradiation campaigns. This would allow multiple entities to obtain the data they require without shouldering the full financial burden associated with such a campaign.

During the first day of the meeting, ORNL and INL participants presented various topics related to the requirements for irradiation campaigns, including ASME code requirements, general discussions about how to perform an irradiation campaign (at ORNL or INL), overviews of the two research reactors (High-Flux Isotope Reactor [HFIR] at ORNL and ATR at INL), and laboratory capabilities for pre- and post-irradiation materials property measurements. The second day started with tours around ORNL including HFIR, the Irradiated Materials Examination and Testing hot cells, and the Low Activation Materials Development and Analysis laboratory. The remainder of the second day was devoted to an open discussion with all attendees.

Open discussion topics ranged from concerns related to graphite shipment due to the non-proliferation treaty, lead times for graphite production, graphite-production capacity limits, and demands for high-purity graphite outside of nuclear. Reactor designers postulated future graphite-irradiation data needs. The primary needs that overlapped with multiple designers included low-dose creep data at 300°C, high-dose (turnaround and cross over) creep data at 450°C, and low-dose high-fidelity data for microreactors. The charge to the participants at the end of Day 2 was to discuss internally future opportunities for collaboration and come prepared to discuss preliminary collaborations during the follow-up workshop. The follow-up workshop is scheduled to be held at INL April 4–6, 2023. The report on the first workshop is being written with the first draft scheduled to go out for review by the end of January.

2.3.6 DOE/EPRI Joint Report

A kickoff meeting was held on December 14, 2022, to discuss roles and responsibilities for the new DOE/EPRI graphite report. This report is intended to provide a status on the use of graphite core components within nuclear applications both from the R&D (DOE) and commercial-designers (EPRI) perspectives. The scope is intended to present less emphasis on material properties and graphite response during nuclear applications and more on technical readiness—with a specific intent to identify technological gaps—in using graphite for HTR applications. An initial outline of the report was established, roles and responsibility were assigned, and a preliminary due date of August 15, 2023, was scheduled.

2.3.7 ASME and ASTM Industry Consensus Development

2.3.7.1 NRC/ASME Engagement

A significant issue was raised by the DOE in their assessment of ASME BPVC HHA code rules concerning the conservatism of the simple-assessment analysis as compared to the full assessment. The question raised a potential issue concerning the calculations for the simple stress limits, Sg. The use of the ratio of flexural to tensile strength (Rtf) parameter to increase the stress limit does not appear to be consistent with the conservatism built into the ASME code rules. This issue was referred to the ASME Nonmetallics Working Group for further clarification and resolution. The issue will be brought up at the next ASME code week on February 6-10, 2023.

2.3.7.2 ASME BPVC Section 3, Division 5 Code Status

The last 2022 quarterly meeting of the ASME NDM WG was held in Pittsburgh on November 1, 2022. The WG General Requirements for Graphite and Ceramic Composite Core Components and Assemblies (GCCCCA) was held virtually on Oct 31, 2022, per WG member request.

As the publishing date for ASME Sec III, Div. 5, 2023 edition nears, the general focus for the WGs is to finalize the open ballots and records items for review by Sec III and the Standards Administrative Review Board so that those revisions can be included in the 2023 edition.

Several records passed final review and are on route for 2023 edition. This includes records 20-1307, Proposal for C-C nonmandatory appendices; 20-1308, Simple assessment and Weibull notations, which also includes the split-off errata record 20-2099; and R21-728 (HHB corrections). All were approved by Sec III after the second-iteration review. Record 22-516, Intent on historical use, was revised and recirculated for Sec III review.

Record 22-1463, which clarifies roles and responsibilities, was submitted for next-level review to subgroups General Requirements and High Temperature Reactors. It is unlikely that this record revision will be included in the latest edition.

Between Code Week meetings, several task groups met on a regular basis, including the Composites Task Group, Nonmetallic Component Degradation and Failure Monitoring Task Group (official ASME Task Group under Sec XI), and the Design Task Group. Activities within the Molten Salt and Irradiation Task Groups are also picking up.

2.3.7.3 ASME Task Groups

ASME activities have significantly increased this year. This is seen in participation in the ASME Boiler and Pressure Vessel Code Weeks (ASME BPVC 2020) and associated task groups. NDM (SG-HTR, BPV III) WG meetings took place in November. In addition, Section XI, Division 2 Subgroup and Section XI, Division 2 monitoring and nondestructive examination (MANDE) WG meetings have been convened as an initiative to address RIM requirements for nonmetallics.

The Composite Task Group had a meeting on Oct 27, 2022, and the focus for this meeting was on material versus component modeling and application during design. It was presented by Materials Research & Design, Inc. (MR&D) with very good questions and observations from the community in context of the code. Also, the first draft from MR&D was received and is currently under review. It will support the final report to address the initial analysis that was performed for Sec III, Div. 5, Subsection HH Subpart B. Moreover, the initial analysis of the ASME code rules for Subsection III, Div. 5, HHB for current HTR's will be presented at the 47th International Conference and Expo on Advanced Ceramics and Composites (ICACC 2023) at Daytona Beach during week of January 22–27, 2023. The next task group on composite will be held on January 19, 2023, and the next WG meetings will be held during the ASME BPVC committee meetings scheduled the week of February 5–9, 2023. The meetings will be held virtually.

The Design Task Group met in person in November for discussion on volume grouping and mesh convergence. There was a demonstration of the NDMAS portal. Also, irradiated and unirradiated data spreadsheets were posted to Box for convenient access. INL, MPR Associates, and USNC participants are meeting regularly regarding subtasks. Industry relations and involvement continue with feedback provided on work at Radiant Nuclear on analyses and papers developed at MPR, answering data requests from Kairos and fielding inquiries regarding data access and testing from Westinghouse and Derek Tsang.

The Graphite Molten Salt Reactor (MSR) Task Group lead has been working to draft and finalize the report concerning the Graphite-Salt Interactions Workshop held in July 2022. The workshop had participation from MSR vendors, national labs, DOE, NRC and academia. The workshop elevated vendor concerns related to exposed graphite as a degradation mechanism. The report will compile presentations made by participants and a summary of the issues discussed and recommendations.

2.3.7.4 ASTM Activities

Subcommittee D02.F, Manufactured Carbon and Graphite Products, met in November. The subcommittee's chair and secretary have been managing a strategy for addressing historical ASTM noncompliant standards (according to updated ASTM regulations) to prevent their withdrawal. This includes a new interlaboratory study to support updated standards for the measurement of ash content and moisture in manufactured graphite. Standards for density measurement are under review for fitness for purpose; the existing standards are outdated. Links between ASTM and ASME are receiving attention to ensure consistency, and the initiative to include graphene within the subcommittee is progressing with a materials specification under consideration.

2.3.7.5 ASTM Special Technical Publication 1639

The ASTM symposium, Graphite Testing for Nuclear Applications: The Validity and Extension of Test Methods for Material Exposed to Operating Reactor Environments, was held as a 2-day virtual event on September 23–24, 2021. The preparation and peer review of papers arising from this symposium are complete, and the compilation of papers under STP 1639 was published by ASTM in December 2022 (Figure 21). This book can be downloaded (in color, as a collection, or by individual chapters) and is available in hard copy (with figures in grayscale only) at https://www.astm.org/stp1639-eb.html.

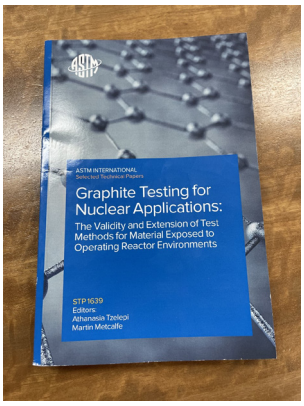

Figure 21. ASTM STP 1639, "Graphite Testing for Nuclear Applications: The Validity and Extension of Test Methods for Material Exposed to Operating Reactor Environments" released online and in print in December 2022.

Five chapters were provided by ART Graphite research staff:

- A. A. Campbell, A. A. Wereszczak, J. W. Geringer, and Y. Katoh, "Equibiaxial Flexure Strength of a Superfine-Grained Nuclear Graphite," pp. 18–33. This chapter introduces the use of advanced ceramic standard, ASTM C1499-05, as the foundation for strength testing of irradiated graphite where sample size is constrained by space limitations in test reactors and large sample sets are not possible. The results suggest an avenue to investigate irradiation-induced changes to the Weibull characteristic strength with a reduced sample population.

- J. B. Spicer, J. D. Arregui-Mena, C. I. Contescu, and N. C. Gallego, "Effects of Microstructural Composition, Porosity, and Microcracks on the Elastic Moduli of Nuclear Graphites," pp. 34–53. This work shows how that many elastic-moduli measurements in nuclear graphite can be modeled in terms of the effects of porosity and microcracking and suggests that similar microstructure-related effects may result from neutron irradiation.
- N. C. Gallego, C. I. Contescu, and R. M. Paul, "Evaluating the Effects of Molten Salt on Graphite Properties: Gaps, Challenges, and Opportunities," pp. 201–221. This primer on testing methods to support graphite use in MSR applications identifies the current state of standards and their fitness for purpose. Distinctions are drawn where existing standards meet or mismatch MSR technology needs by comparison to those relevant to gas-cooled reactors.
- R. M. Paul, C. I. Contescu, and N. C. Gallego, "A Microstructural Modeling-Based Approach to Graphite Oxidation beyond ASTM D7542," pp. 257–278. This work outlines the development of the random-pore model to describe the oxidation mass-loss rates associated with IG-110, PCEA, and NBG-18. While the ASTM D7542 standard emphasizes the collection of reproducible oxidation data for the extraction of kinetic parameters, this model connects the rate data to the graphite microstructure and the subsequent analysis highlights issues with achieving uniformly oxidized specimens necessary for meaningful post-oxidation determination of thermal and strength properties.
- R. E. Smith, and W. E. Windes, "Performance of Graphite Oxidation with Environment and Specimen Geometry Variations," pp. 279–303. This study compares observed oxidation performance between geometries and practices described in ASTM D7542 and parallel smaller-scale testing using a TGA. Practical observations are described to highlight and constrain the extrinsic parameters that influence graphite oxidation as an expression of the intrinsic graphite material characteristics.

2.3.8 Upcoming TMS Meetings

The upcoming annual TMS meeting will be held March 19–23, 2023 (TMS2023 Homepage) and includes a symposium entitled "Composite Materials for Nuclear Applications II" (Symposium Information). Anne Campbell (ORNL) is the lead organizer for this symposium. The Tuesday afternoon session of this symposium is titled "Graphite/Carbon Composites" and includes an invited talk to be presented by W. E. Windes (INL) and T. J. Gerczak (ORNL), contributed talks from J. D. Arregui-Mena and A. A. Campbell, and a contributed talk from North Carolina State University on fission-product diffusion in graphite (Nuclear Energy University Project, Consolidated Innovative Nuclear Research funding), and a contributed poster from S. D. Johns. This will be the second occurrence of this symposium (the first was in 2021). Given the interest and participation in both events, the plan is to make this a recurring symposium offered in odd years.

The date and location for the Materials in Nuclear Energy Systems (MiNES) 2023 meeting has been set for December 10–14, 2023 in New Orleans, LA. Anne Campbell (ORNL) is serving as the technical chair for this meeting (and serving as general chair for the 2025 meeting). The MiNES meeting occurs every two years, and sponsorship alternates between TMS and the ANS. The aim of the MiNES meeting is to bring together researchers from the fission reactor-materials and fuels areas to discuss the latest progress. There has been a strong representation of the DOE ART work in TRISO and compacted fuel, and with the 2023 meeting Campbell is actively working to increase participation with the nuclear graphite research community.

2.3.9 GIF Status

The next GIF VHTR Materials PMB meeting will be held in Manchester, UK, on April 18–21, 2023. The PMB committee has requested that DOE ART organize a special session on graphite-molten salt based upon our experience in this area of research. Dr. Nidia Gallego and Will Windes have volunteered to assist in organizing, as well as participating in, this special session of the GIF PMB meeting.

For more information, contact:

Researcher	Expertise
Andrea L. Mack andrea.mack@inl.gov	ASME Code
Anne Campbell campbellaa@ornl.gov	PIE, Irradiation damage, Irradiation behavior
Arvin Cunningham arvin.cunningham@inl.gov	Oxidation, Split-disk testing
Austin C. Matthews austin.matthews@inl.gov	Material property testing, PIE, Oxidation
David T. Rohrbaugh david.rohrbaugh@inl.gov	Unirradiated and Irradiated material properties
Jose' D. Arregui-Mena arreguimenjd@ornl.gov	Microstructure, irradiation damage
Lu Cai Lu.Cai@inl.gov	Pebble Oxidation
Martin Metcalfe martin.p.metcalfe@gmail.com	HTR operations, ASME, ASTM

Researcher	Expertise
Mary Kaye Aimes marykaye.ames@inl.gov	Oxidation, Material testing
Michael E. Davenport michael.davenport@inl.gov	Irradiation experiments
Nidia C. Gallego gallegonc@ornl.gov	Molten salt technical lead, irradiation damage
Philip L. Winston philip.winston@inl.gov	Irradiation experiments
Rebecca E. Smith rebecca.smith@inl.gov	Graphite oxidation (irr. and unirr)
Steve Johns Steve.johns@inl .gov	Irradiation damage, Characterization, Split-disk
William Windes william.windes@inl.gov	Irradiation behavior, ASME
Wilna Geringer geringerjw@ornl.gov	ASME, Composites, Graphite

2.4 Methods Modeling and Validation

2.4.1 Publications, Audits, Reviews

2.4.1.1 NSTF Test Campaign

The NSTF program team held a 1-day review meeting at ANL on December 13th, 2022, to present recently completed testing and simulation results, and then jointly discuss the path forward remaining water-based matrix testing. The team invited others involved with the NSTF/RCCS effort to include their participation and updates on their work. The final attendance included 25 meeting participants: six virtual and 19 in person. Represented at the meeting were federal, regulatory, and national lab participants (ANL, DOE, NRC, and INL), four industry vendors (Framatome, X-Energy, Kairos, and Boston Atomics), and two US universities (University of Wisconsin–Madison and Texas A&M University). Meeting minutes were documented and have been included in the NSTF program records. Presentations from ANL and the two guest speakers are being compiled for distribution and will be transmitted to the meeting participants by early January 2023. The collaboration of industry, federal, national labs, and universities will provide the necessary support needed to make the water NSTF program, and the overall US industry passive decay-heat removal initiative, a success.

The NSTF Program team extended an invitation for a formal external audit of the Quality Assurance Program Plan for NQA-1 compliance. The program typically performs management assessments every 6 months, formal internal audits every 12 months, and formal external audits every 18–24 months. With the last external audit in the spring of 2021, the program is coming due for another visitation. Thus, an invitation letter was sent to INL requesting an audit in February of 2023. For this FY-23 audit, the INL Checklist (INL PDD-13000, Rev. 10) will be used to identify quality requirements, with evaluation metrics limited to only those elements pertaining to the graded approach described in the latest revision of ANL-NSTF-000000-ADMIN-007 and will cover only the 2008/1-2009a edition of NQA-1. With the invitation letter requested by the program manager, planning is underway for the audit, including reservation of conference spaces, coordination with team members, and discussions with the lead auditor on required documentation and time frames for transmitting the records.

Three members of the NSTF team attended the 2022 ANS Winter Meeting in Phoenix, Arizona. One presented a paper entitled “Modeling of a Large Scale RCCS Operating at Two-Phase Transient

Conditions with RELAP5-3D," while another presented as a panel speaker during the Thermal Hydraulics Issues in Licensing of Advanced Reactors session. Included in this panel talk were the validation activities performed as part of the NSTF experimental program.

The preparation of a conference paper for submission to NURETH-20 was initiated.

2.4.1.2 Modeling and Simulation

One member of the Advanced Reactor Modeling and Simulation group and one collaborator (a summer intern) from Pennsylvania State University presented four papers at the 2022 (ANS) Winter Meeting in Phoenix:

- "Methodology for Determining the Run-In Scenario for a Pebble Bed Reactor"
- "Discrete Element Method Investigation of Reflector Dimples for a General Pebble Bed Reactor Design"
- "Gas Cooled Reactor Equilibrium Core Calculations Using NEAMS Tools"
- "Determination of an Initial Critical Fuel Height for a Pebble-Bed Reactor."

A journal paper was submitted to *Annals of Nuclear Energy* with title "Improved Multiphysics Model of the High Temperature Engineering Test Reactor for the Simulation of Loss-of-Forced-Cooling Experiments." The comments from two reviewers were addressed, the paper was modified accordingly, and both extra content and references requested were added. In addition, an abstract was submitted and accepted for the M&C 2023 Conference: "Preliminary Sensitivity Analysis for the Validation of High Temperature Test Reactor Transient Simulations."

A journal paper was submitted to *Annals of Nuclear Energy* with title "Discrete Element Simulation of Pebble Bed Reactors on Graphics Processing Units." The comments from two reviewers were addressed, adding a sensitivity study on the dimension of the pebble-bed dimples.

A journal paper has been drafted for submission to *Annals of Nuclear Energy* with title "High-Fidelity Monte Carlo based simulation of a Pebble Bed Reactor the Run-In phase."

2.4.1.3 HTTF Benchmark

Presented HTTF work, "Assessing the Impact of Effective Thermal Conductivity on Gas-Cooled Reactor Transients in RELAP5-3D," at the 2022 ANS Winter Meeting, Phoenix, November 13–17, 2022.

Presented benchmark participants overview at G4SR: "Overview of HTTF Modeling and Benchmark Efforts for Code Validation for Gas-Cooled Reactor Applications", *Proceedings Fourth International Conference on Generation IV & Small Reactors (G4SR-4), Toronto, ON, Canada, October 3–6, 2022*.

Submitted journal paper "High Temperature Test Facility sensitivity and calibration studies to inform OECD-NEA benchmark calculations" on Digital Calibration Certificate, describing sensitivity and calibration studies conducted for HTTF using RELAP5-3D to *Nuclear Engineering and Design*.

2.4.2 Experimental Activities for Code Validation

2.4.2.1 NSTF Test Campaign

The experimental team performed one successful matrix test during the reporting period, DataQuality 079, which looked at a specific mid-range power level with an aim to identify a delineation point between two families of instability modes previously observed. The baseline two-phase cases have been performed at the full-scale accident-power decay-heat load of 2.1 MWt while the single-phase normal-operation testing is performed at 1.4 MWt of decay-heat load. The latest test was performed at a middle range of 1.8 MWt and identified a transitional mode of operation that did not exhibit a predictable or consistent behavior trends otherwise observed with the higher- or lower-power cases, Figure 22. A data review was completed, allowing the team to issue a preliminary test-acceptance report; however, data analysis and understanding of the phenomena are still ongoing.

The team also completed an additional matrix test, DataQuality 081. This test case revisited the condition of operating until inventory depletion to examine methods for inventory refill. The method for this test was a best attempt to reflect what a full-scale plant would see in an accident scenario: high flow rate refill of cold inventory directly into the upper dome of the tank. Several provisions were made to allow use of the high flow pump, including new routing within the laboratory and mezzanine structure. Scoping trials were first performed and indicated that the loop could be replenished post-depletion with the ~350 gallons needed to return the level back to the tank inlet in a period of ~25 minutes. Prior test cases used a significantly lower refill flow rate, during which violent geysering phenomena were observed due to the stagnant fluid in the heated section. DataQuality 081 began on November 30 and was successfully completed by December 1. Heating of the loop spanned approximately 11 hours, at which point boiling was established, and the loop entered a regime of stable two-phase flow. After approximately 6 hours past boiling, flow stagnation occurred as the loop experienced an abrupt cessation of flow. Three discrete geysering events were allowed to occur, after which point the cold refill was initiated. During the roughly 25-minute cold refill period, two additional geysering events were witnessed, a significant reduction compared to previous low-flow cases (Figure 23). Accelerometers were used to measure the impact of flow vibrations and measured nearly 2g’s of vibrational forces on the chimney piping, metal structures, and primary tank.

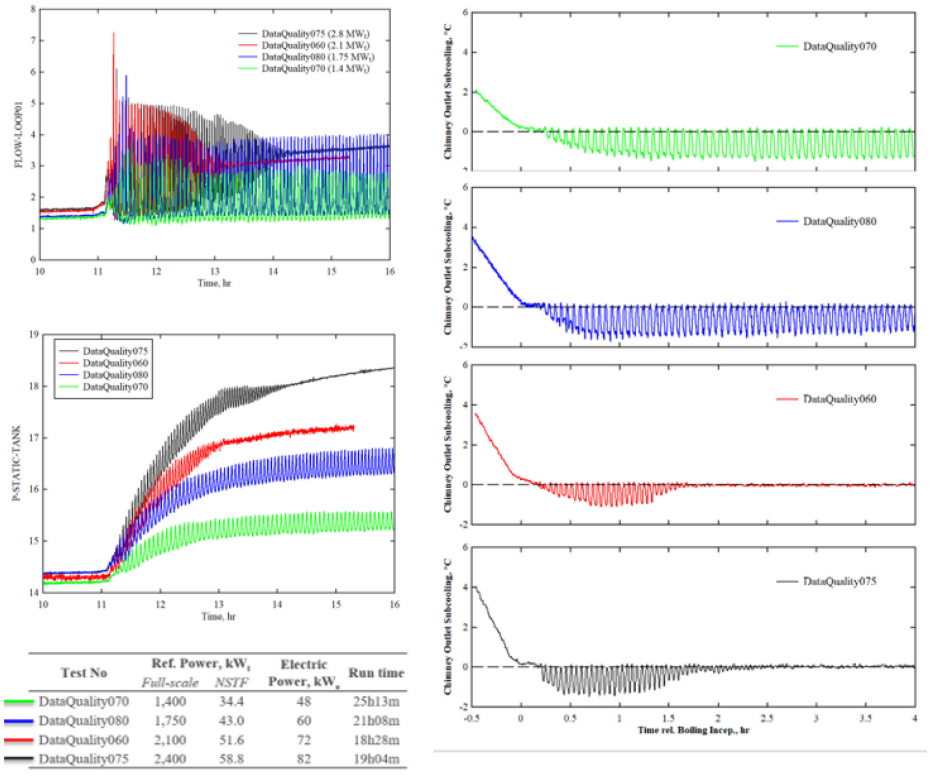

Test No	Ref. Power, kW_t *Full-scale*	Ref. Power, kW_t *NSTF*	Electric Power, kW_e	Run time
DataQuality070	1,400	34.4	48	25h13m
DataQuality080	1,750	43.0	60	21h08m
DataQuality060	2,100	51.6	72	18h28m
DataQuality075	2,400	58.8	82	19h04m

Figure 22. Comparison of flow rate, gas pressures, and chimney subcooling for power parametric.

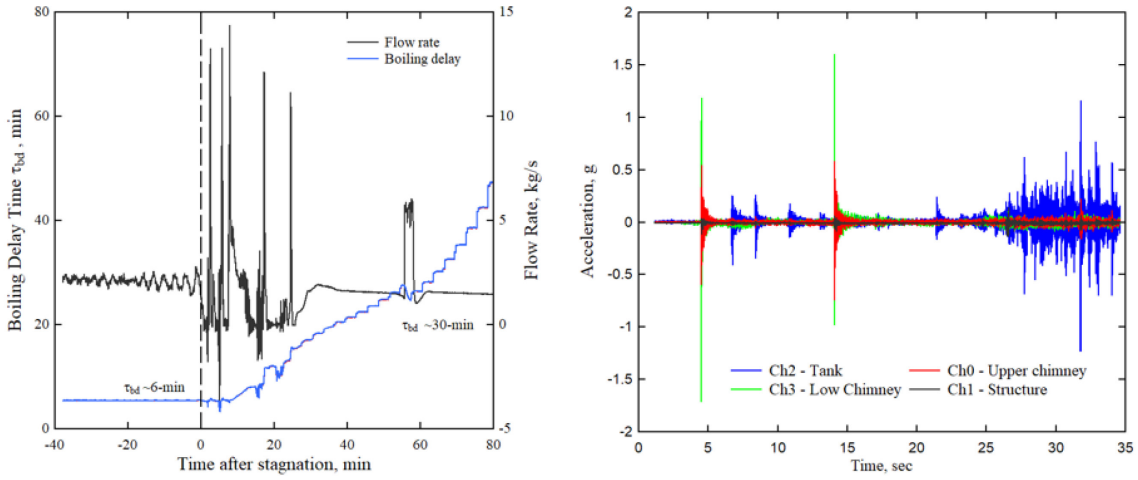

Figure 23. Geysering events during flow-depletion test case.

Following conclusion of the meeting, and in preparation for the extended holiday break and laboratory shutdown, the experimental team placed the test facility into warm standby. Activities included draining all the inventory from the test loop, powering off the high-voltage feed systems, enabling remote-monitoring checks, and changing water filters in the storage tanks.

2.4.2.2 HTTF benchmark

We compiled results from the code-to-code comparison problems of the benchmark. An example of those results is available in Figure 24, which contains temperatures at the core midplane for a pressurized conduction-cooldown transient initiated from full-power steady state. These results correspond to Problem 3 Exercise 1B of the benchmark.

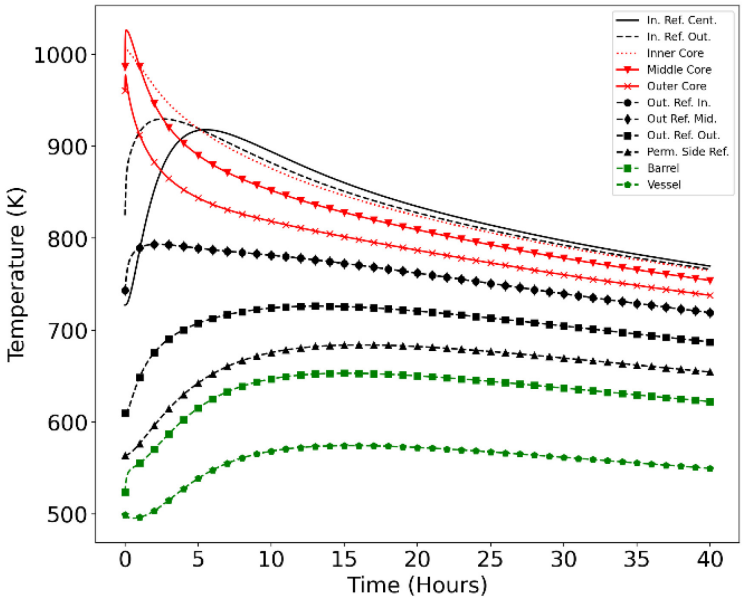

Figure 24. Temperatures at the core midplane of the HTTF during a pressurized conduction cooldown.

2.4.3 Modeling and Simulation

2.4.3.1 NSTF Test Campaign

The computational and simulation work performed in FY-22 was presented at the NSTF Program Review Meeting held at ANL. In areas of modeling efforts, the RELAP5-3D model of the NSTF continued to be refined and updated. Studies were performed to investigate the effects of chimney-heat loss and tank-gas space pressure on the accuracy of the model. It was shown that by tuning the chimney-heat loss, the model could better predict the onset and duration of two-phase instability. The model was also benchmarked with a transient condition with blocked riser channels where the prediction appeared to agree reasonably well with the experimental data.

2.4.3.2 Monte Carlo Based Run-in Methodology

As shown in Figure 25, a sensitivity analysis on dimple geometry was performed, as requested by one of the reviewers, during the publication process of the related journal. The calculation demonstrated that after 0.5 times the diameter of the pebbles, the effect on porosity is negligible. New pebble-bed partition coming from the previous study was implemented (including dimples) in the Monte Carlo model as shown in Figure 26. Three different run-in cases were studied using a new control-logic capable of predicting the excess reactivity and adjust the recirculation rate to maintain the k-eff around the desired value, as shown in Figure 27. The effect of temperature feedback and control rod insertion was studied. The control logic reduces sensibly the discharge burnup to a value closer to the one published in open-source literature of 164 MWd/T_{HM}.

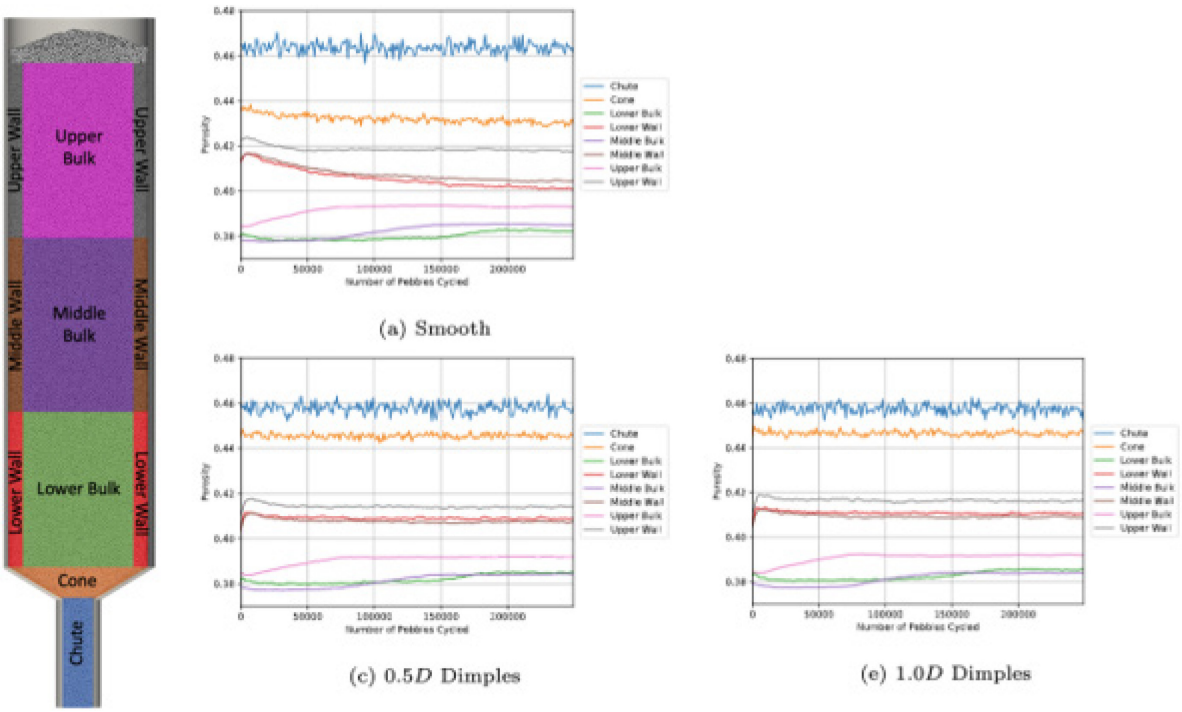

Figure 25. Sensitivity analysis of the dimples geometry on the local porosity of the pebble bed.

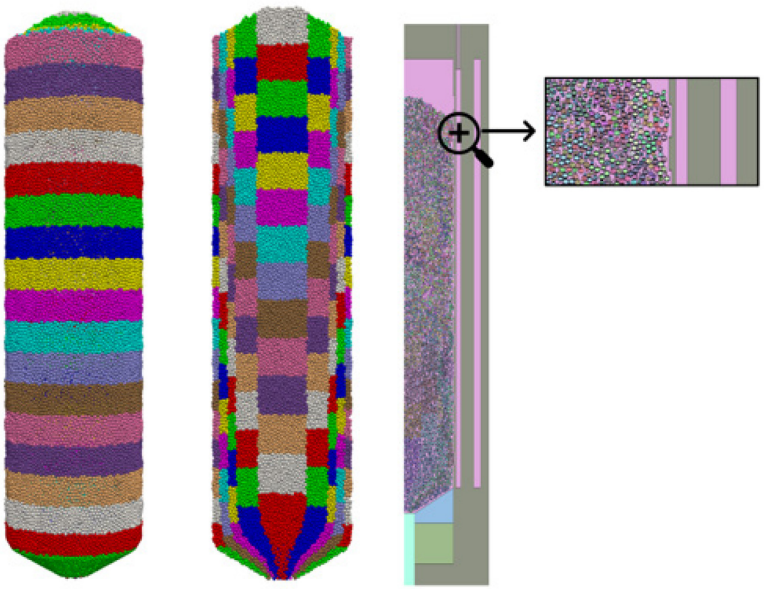

Figure 26. Sensitivity analysis of the dimples geometry on the local porosity of the pebble bed.

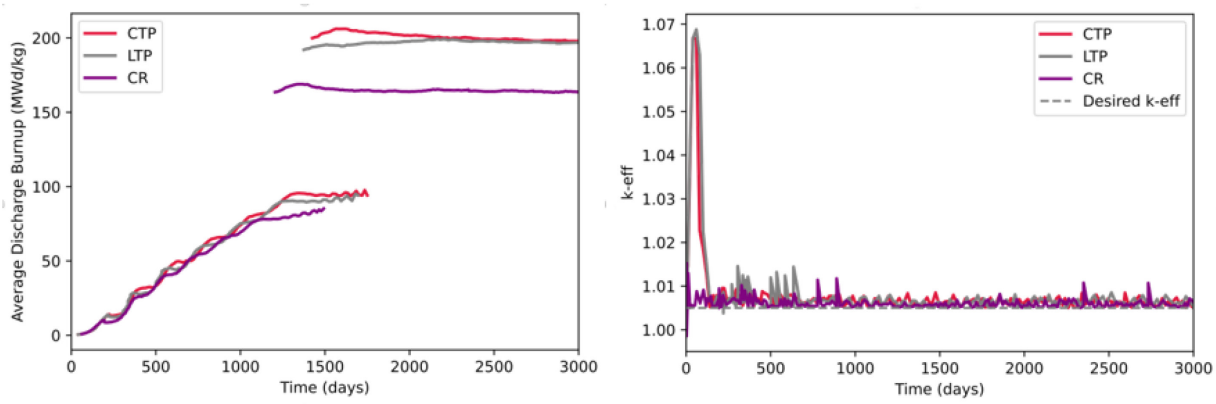

Figure 27. Three different run-in cases (constant and linear temperature and linear temperature with control rods in), average discharge burnup, and k-eff, using new pebble-recirculation control logic.

2.4.3.3 Deterministic Equilibrium Core Calculations Optimization Studies

During the first quarter of FY-23 a new mesh for the gPBR200 model to accommodate the streamlines calculated using project chrono software was generated using Multiphysics Object Oriented Simulation Environment (MOOSE) modules (see Figure 28). The Pronghorn model was modified to be able to use the finite-volume method discretization to increase stability and flexibility. Null transient restart from the steady-state equilibrium core calculation was successfully tested.

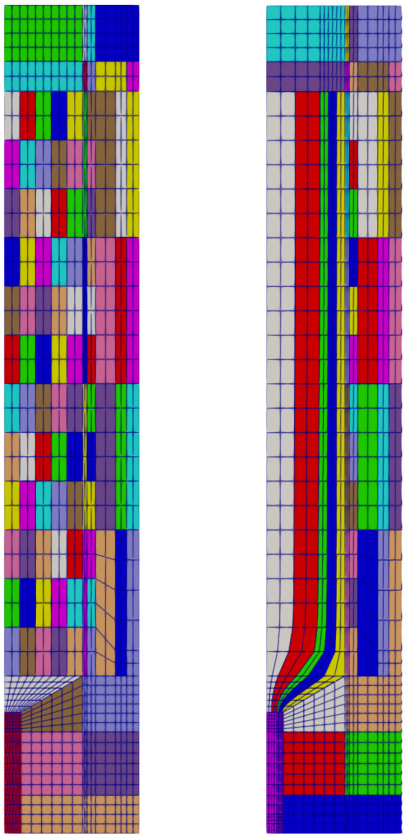

Figure 28. Old griffin regular mesh (left) and new griffin mesh to accommodate streamline geometry (right).

2.4.4 International Collaborations

2.4.4.1 HTTF Benchmark

The first draft of HTTF benchmark specifications have been completed and submitted to the OECD-NEA for their review.

2.4.4.2 HTTR LOFC Benchmark

The multiphysics model of HTTR developed to validate the NEAMS tools against past and future loss-of-forced-cooling (LOFC) experiments (final test in 2023) was improved. The time and magnitude of the first power peak after recriticality is now predicted within 1.5 hours and 175 kW, respectively. The last modeling approach selected combines 3-D full-core super-homogenization-corrected neutronics, a new 3-D full-core semi-heterogeneous heat transfer (macroscale), a new two-dimensional (2-D) axisymmetric fuel-rod heat transfer (at pin-scale), relying on gap conductance, and 1-D thermal-hydraulics channels. The new macroscale/pin-scale heat-transfer coupling approach relying on gap conductance drastically sped up (by two orders of magnitude) numerical convergence. The semi-heterogeneous model (see Figure 29) improved the recriticality time discrepancy, reducing it to less than 1 hour (see Figure 30). Most importantly, the initial recriticality observed in the first 15 min of the transient, using the homogeneous mesh and not measured in the reactor, is not present in the calculations with the semi-heterogeneous thermal conduction model.

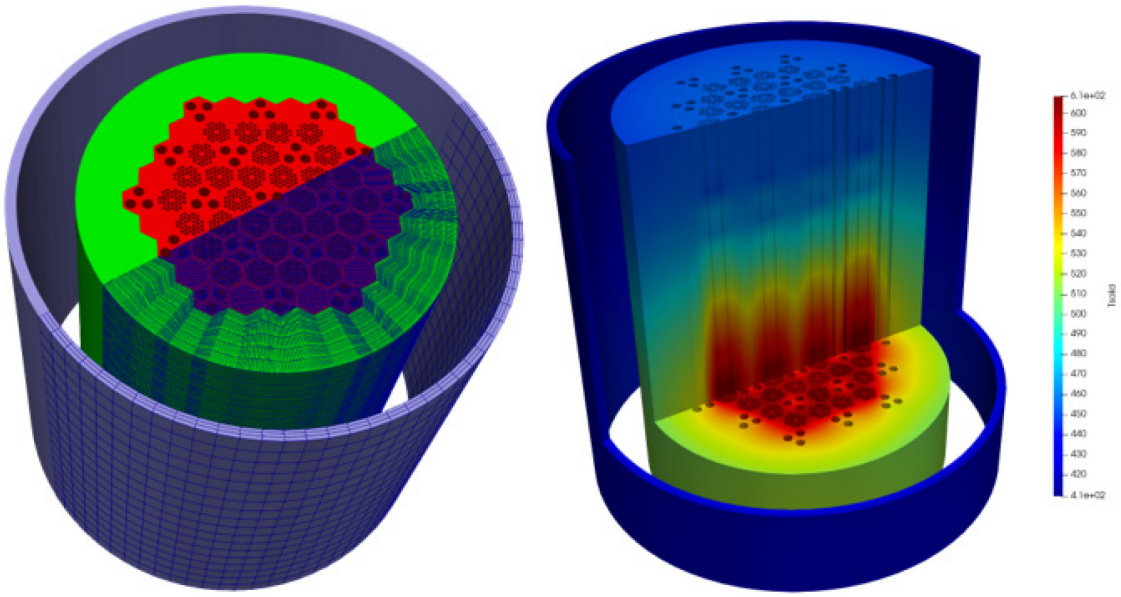

Figure 29. HTTR semi-heterogenous mesh generated with the MOOSE reactor module (left) temperature distribution obtained using the same mesh (right).

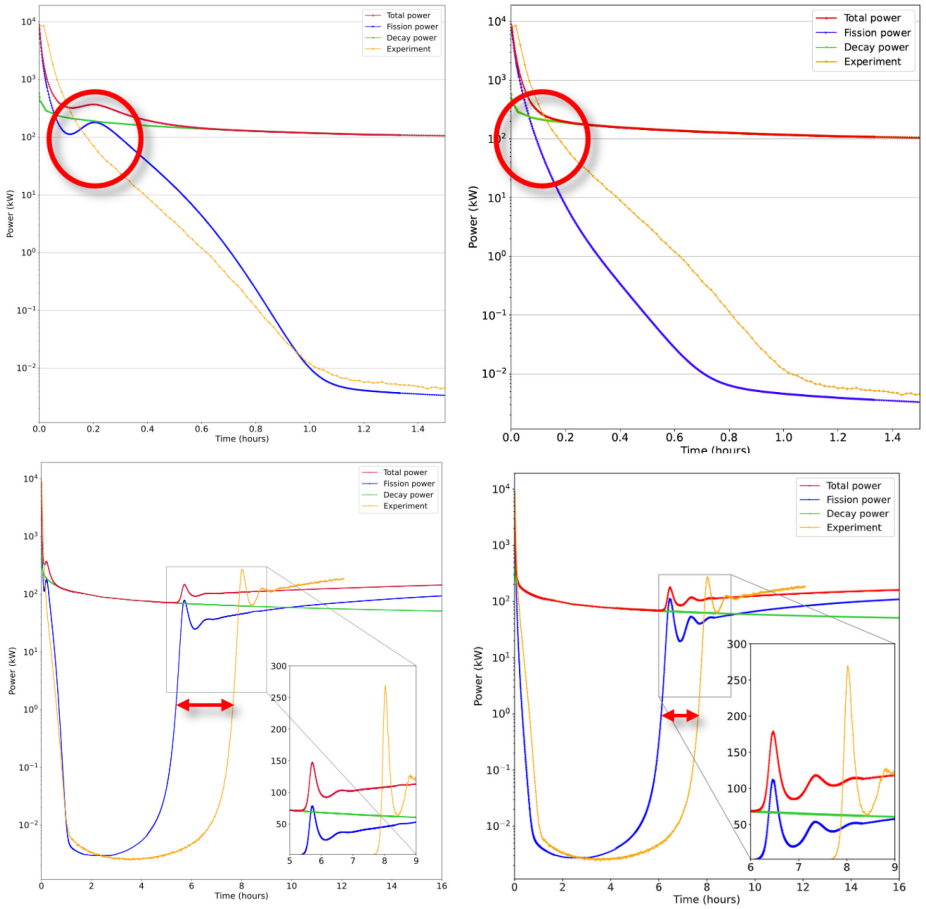

Figure 30. Improvement on the results using the semi-heterogenous thermal conduction model. Old results (left) new results (right).

2.4.4.3 Civil Nuclear Energy Research and Development Working Group

The group drafted and submitted to the Japan Atomic Energy Agency (JAEA) the 3-year extension of the bilateral collaboration between US and Japan. Coordinating the validation efforts among the two countries, using both HTTR and HTTF data as key elements, will guarantee a broader understanding and assessment of the phenomena occurring during normal operation and accident phase of prismatic HTGRs. The power operation of HTTR will provide invaluable data on coupled neutronic/thermal-fluid transients that can be used for multiphysics code validation when the tests from the HTTF (highly instrumented) will provide a deeper understanding of the heat-transfer mechanisms in the core during accidental conditions. The new work scope includes four tasks, three of which regard HTGR modeling and simulation activities based on HTTR and HTTF data, and the last is undertaken by the Integrated Energy System Program. The first task, Data, Models, and Codes Exchange, will ensure that both the country share data, models, and codes following the licensing and access procedures of the country that host it. The second task, Tritium Generation and Transport Modeling Validation, will use tritium measurement data during power operation of HTTR to validate MELCOR (for melting core) for high-temperature reactors. The last task, Multiphysics Reactor Dynamics Modeling Validation, will leverage the existing models developed using the NEAMS tools for the LOFC benchmark, adding a control-rod model and validating them using the control-rod's positions, power (See Figure 31), and temperature measurements.

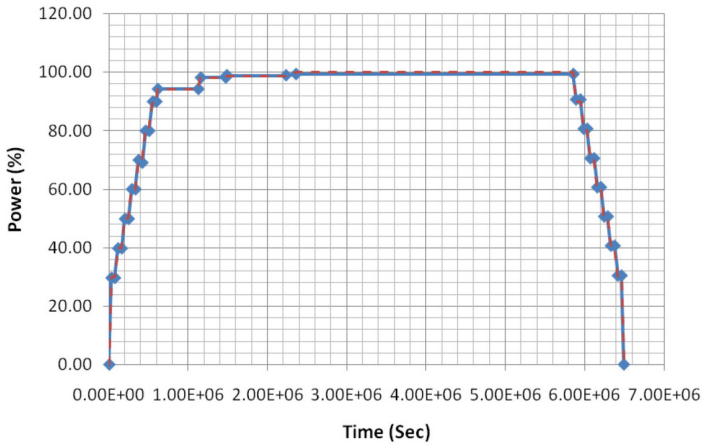

Figure 31. Ramping up of HTTR power from zero to full power and back to zero in 1800 h.

2.4.4.4 GIF

After the signatory on November 30th initial activities for the tasks lead by the DOE were performed. In the framework of Task 1.1, extensive study of the NGNP Phenomena Identification and Ranking Table (PIRT) to generate a template for the comparison with the PIRTs from the other country members was performed.

For more information, contact:

Paolo Balestra (paolo.balestra@inl.gov)

Darius Lisowski (dlisowski@anl.gov)

Aaron Epiney (aaron.epiney@inl.gov)

3. 90 DAY LOOK AHEAD

3.1 Fuels Development

- Complete electron microscopy of particle cross-sections from AGR-5/6/7 Compacts 1-7-9 and 1-7-4 at INL
- Prepare additional AGR-5/6/7 Compact 1-7-9 particles that were previously examined via X-ray for analysis via electron microscopy at INL.
- Assess the feasibility of sending entire AGR-5/6/7 compacts from HFEF to the IMCL for XCT at INL.
- Assess the feasibility of sending AGR-5/6/7 compact cross-sections (especially mounts of Compact 1-6-9) from HFEF to IMCL for electron microscopy at INL.
- Perform 1600°C safety test on AGR-5/6/7 Compact 3-1-2 with ORNL CCCTF.
- Complete LBL of AGR-5/6/7 Compacts 1-5-9 and 4-1-3 at ORNL.
- Complete gamma counting of TRISO particles from AGR-5/6/7 Compacts 1-5-9 and 4-1-3 at ORNL.
- Complete SEM at ORNL of irradiated TRISO particles from AGR-5/6/7 Compacts 2-2-1, 2-2-2, and 2-2-4.
- Complete axial gamma scanning of the AGR-5/6/7 Capsule 5 graphite holder using the PGS at INL.
- Complete gamma tomography of the AGR-5/6/7 Capsule 2 holder via PGS at INL.

- Complete axial gamma scanning of the AGR-5/6/7 Capsule 4 graphite holder via PGS at INL.
- Complete ceramographic preparation and optical microscopy of three mounts of particles from AGR-5/6/7 Compact 1-7-9 and four mounts of particles from Compact 1-7-4 at INL.
- Complete the Phase IIA qualification plan for the Air/Moisture Ingress Experiment and start integrated testing of all its systems.
- Complete a Level 3 milestone for the radiochemical analyses of the samples from the destructive sampling of the AGR-3/4 Capsule 4 inner and outer rings at INL.
- Complete a Level 2 milestone report on AGR-5/6/7 disassembly and initial non-destructive examinations at INL (often called the "first look" report).
- Complete a 300-h, 1600°C test of AGR-5/6/7 Compact 4-4-4 in the Fuel Accident Condition Simulator furnace at INL.
- Begin using a new stage for the Visual Examination Machine at INL for examinations of AGR-5/6/7 compacts prior to shipment to ORNL and prior to use in other non-destructive PIE work.

3.2 High-Temperature Materials

- High-Temperature Design Methodology—INL
  - Continue the development of the new Class B design rules.
- Long-Term VHTR Material Qualification—INL
  - Alloy 617 double V-notch specimen from a recently completed test will be characterized via microscopy (rupture notch) and X-ray CT (unruptured notch).
  - Two new 617 double V-notch tests will be started, with planned interruption times for X-ray CT measurements. One will be at 800°C, 65 MPa, and the other at 850°C, 63 MPa.
  - Integrate a new motion controller to get the gas tungsten arc-welding equipment operational to produce qualification welds using UTP A 2133 Mn filler wire on Alloy 800H plate. The motion controller was ordered, but delivery has been delayed until March 30th. Alternate welding routes are being explored to ensure work progresses.
  - Perform the Alloy 800H qualification welds with the UTP A 2133 Mn filler wire using semi-automated gas tungsten arc welding. This qualification will be in accordance with Section IX of the ASME BPVC. An INL procedure-qualification record and welding-procedure specification will be qualified to support these welds.
  - Machine specimens for creep crack growth rate testing.
  - Perform calibration testing on fatigue cracks to determine the accuracy of DCPD measurements at determining crack growths *in situ*.

3.3 Graphite Development and Qualification

- Finish editing of the manuscript entitled "High Temperature Annealing of Irradiated Nuclear Grade Graphite" for acceptance for publication in the *Journal of Nuclear Materials*.
- Begin graphite TEM analysis at the MFC and CAES.
- Complete installation of *in situ* heating holder on the Spectra TEM at CAES.
- Complete report on baseline material-property testing of 4th PCEA billet by February 1, 2023.
- Complete report on baseline material-property testing of 5th PCEA billet by March 1, 2023.
- Complete status memorandum on ASTM standards development by March 1, 2023.

3.4 Methods Modeling and Validation

- Return from holiday break and return facility to service.
- Continue matrix testing along the planned off-normal or blocked scenarios.
- Host NQA-1 lead auditor from INL in February for NQA-1 audit of NSTF Quality Assurance Program Plan.
- Finalize publication of HTTF journal article for *Nuclear Engineering and Design*.
- Aaron Epiney traveling to OECD-NEA meeting in Paris.
- Finalize plans for the benchmark kickoff meeting.
- Present methods work to JAEA representative visiting INL.
- Attend the LOFC Benchmark meeting to provide an update on the results and obtain new data.
- Attend the Civil Nuclear Energy Research and Development WG meeting to finalize the activity extensions.
- Attend the first official CMVB GIF meeting to kickstart the efforts and coordinate with the other participants.
- Publish discrete-element method and HTTR journal papers.
- Establish collaboration with NRC for the HTTR LOFC benchmark.
- Finalize GIF tasks (mainly literature review and transferring data) due in 6 months after the signatory of the agreement.
- Reconstruct the volume matrix for transferring data between Pronghorn/Griffin and the Serpent Run-in model.
- Finalize the updates on the GPBR200 Pronghorn/Griffin and perform initial depressurized loss of forced cooling studies.

4. REFERENCES

1. Rice, F. J., J. D. Stempien, and P. A. Demkowicz. 2018. "Ceramography of irradiated TRISO fuel from the AGR-2 experiment." *Nuclear Engineering and Design* 329: 73–81. https://doi.org/10.1016/j.nucengdes.2017.10.010.
2. Wang, Y., Z. Hua, R. Schley, G. Beausoleil II, and D. H. Hurley. 2022. "Thermal properties measurement of TRISO particle coatings from room temperature to 900 °C using laser-based thermoreflectance methods." *Journal of Nuclear Materials* 565: 153721. https://doi.org/10.1016/j.jnucmat.2022.153721.
3. Barnes, Charles Marshall, and Douglas W. Marshall. "FY 2008 Six-inch Diameter Coater Test." INL/EXT-08-14633, Idaho National Laboratory, Idaho Falls, ID. https://inldigitallibrary.inl.gov/sites/sti/sti/7363961.pdf.
4. Barnes, C. M., D. W. Marshall, J. T. Keeley, and J. D. Hunn. 2009. "Results of tests to demonstrate a 6-in.-diameter coater for production of TRISO-coated particles for AGR experiments." *Journal of Engineering for Gas Turbines and Power* 131(5). https://doi.org/10.1115/1.3098424.
5. Sham, T.-L., H. Mahajan, and Y. Wang. 2022. "Initial Development of Variable Design Lifetimes and Creep-Fatigue Evaluations for ASME Section III, Division 5, Class B Code Rules." INL/RPT-22-69139, Idaho National Laboratory, Idaho Falls, ID. https://inldigitallibrary.inl.gov/sites/sti/sti/Sort_63606.pdf.

6. Wang, Y., R.I. Jetter, T.-L. Sham. 2017 "Report on FY17 Testing in Support of Integrated EPP-SMT Design Methods Development." ORNL/TM-2017/351, Oak Ridge National Laboratory, Oak Ridge, TN. https://doi.org/10.2172/1376507.
7. Wang, Y., R.I. Jetter, M.C. Messner, T.-L. Sham. 2019. "Report on FY19 Testing in Support of Integrated EPP-SMT Design Methods Development." ORNL/TM-2019/1224, Oak Ridge National Laboratory, Oak Ridge, TN. https://info.ornl.gov/sites/publications/Files/Pub127918.pdf.
8. Barua, B., M.C. Messner, Y. Wang, T.-L. Sham and R.I. Jetter, 2021. "Draft Rules for Alloy 617 Creep-Fatigue Design using an EPP+SMT Approach." ANL-ART-227, Argonne National Laboratory, Lemont, IL. https://doi.org/10.2172/1819737.
9. Messner, M.C. 2022. "A Viscoplastic Model for Alloy 800H for Use with the Section III, Division 5 Design by Inelastic Analysis Methods for Class A Components." In proceedings of the American Society of Mechanical Engineers Pressure Vessels and Piping Conference, Las Vegas, NV. https://doi.org/10.1115/PVP2022-84861.
10. Arregui-Mena, J. D., D. V. Griffiths, R. N. Worth, C. E. Torrence, A. Selby, C. Contescu, M. Gallego, P. D. Edmondson, P. M. Mummery, and L. Margetts. 2022. "Microstructural characterization data of as received IG-110, 2114 and ETU-10 nuclear graphite grades and oxidation characterization data of IG-110." *Data in Brief*, 44:108535. https://doi.org/10.1016/j.dib.2022.108535.
11. Wang, C, X. Sun, and R. N. Christensen. 2019. "Multiphysics simulation of moisture-graphite oxidation in MHTGR." Annals of Nuclear Energy 131: 483–95. https://doi.org/10.1016/j.anucene.2019.03.040.
12. Ozaltun, H. D. Liepinya, and V. A. Avincola. 2021. "Review of Graphite Properties Relevant to Micro-Reactor Design." INL/CON-21-62450, Idaho National Laboratory, Idaho Falls, ID. https://www.osti.gov/servlets/purl/1812214.
13. "Standard Test Method for Tensile Strength Estimate by Disc Comparison of Manufactured Graphite." ASTM D8289-19. Annual Book of ASTM Standards, ASTM International, West Conshohocken, PA. https://webstore.ansi.org/standards/astm/astmd828919.
14. Burchell, T. D. 2020. "Mersen Grade 2114: A Comparison of Tensile Strength Data." ORNL/TM-2020/1458, ORNL, Oak Ridge, TN. https://info.ornl.gov/sites/publications/Files/Pub137214.pdf.